ISTANBUL TECHNICAL UNIVERSITY ★ GRADUATE SCHOOL OF SCIENCE ENGINEERING AND TECHNOLOGY

POLYSULFONE-BASED AMPHIPHILIC POLYMERS

M.Sc. THESIS

Buket ALKAN

Department of Polymer Science and Technology

Polymer Science and Technology Programme

MAY 2014

ISTANBUL TECHNICAL UNIVERSITY ★ GRADUATE SCHOOL OF SCIENCE ENGINEERING AND TECHNOLOGY

POLYSULFONE-BASED AMPHIPHILIC POLYMERS

M.Sc. THESIS

Buket ALKAN
(515121004)

Department of Polymer Science and Technology

Polymer Science and Technology Programme

Thesis Advisor: Prof. Dr. Metin H. ACAR

MAY 2014

İSTANBUL TEKNİK ÜNİVERSİTESİ ★ FEN BİLİMLERİ ENSTİTÜSÜ

POLİSÜLFON ESASLI AMFİFİLİK POLİMERLER

YÜKSEK LİSANS TEZİ

Buket ALKAN
(515121004)

Polimer Bilim ve Teknolojileri

Polimer Bilim ve Teknolojileri Programı

Tez Danışmanı: Prof. Dr. Metin H. ACAR

MAYIS 2014

Buket Alkan, a **M.Sc.** student of ITU **Institute of Science and Technology/ Graduate School of Istanbul Technical University** student ID **515121004**, successfully defended the **thesis** entitled "**Polysulfone-Based Amphiphilic Polymers**" , which she prepared after fulfilling the requirements specified in the associated legislations, before the jury whose signatures are below.

Thesis Advisor :	**Prof. Dr. Metin H. ACAR** İstanbul Technical University	.....
Jury Members :	**Prof. Dr. Name SURNAME**	.....
	Prof. Dr. Name SURNAME	.....

Date of Submission : 25 April 2014
Date of Defense : 28 May 2014

To my parents,

FOREWORD

This master project was carried out at Istanbul Technical University, Chemistry Department of Science & Letters Faculty, Pol-Merg Laboratory under the teaching supervisor of Prof. Metin H. ACAR, under support of Istanbul Technical University Institute of Science and Technology.

I would like express my deep pride, regards and thanks to my supervisor Prof. Metin H. ACAR for his sincere supervision, advice, and guidance of this study. He supported me during thesis and guided to open my mind for research to look for different views. Through his wealth of knowledge, direction and leadership I have been able to expand my knowledge in many areas of polymer science. It was a great pleasure for me to work with him.

I wish to express my special thanks to C.Erdinç TAŞ, and I also acknowledge to other labmates Ahmet Y. DEMİR, Eren ELİK, Mehmet BAŞDAL, Merve BAYRAKTAR for their friendship, help and support. It was a great pleasure to work with them. Many thank to Giray Ersözoğluları for Impedance measurements.

My sincere thanks go to my friend E. Billur SEVİNİŞ for her endless help, trust and sisterhood. I also would like to thank my friends Aylin ALTINIŞIK, İrem BALKESER and Yasemin FİDAN for all their help and support.

I also want to thank my mother Bedriye ALKAN, my father Sinan ALKAN and my brother B. Uygar ALKAN for their patience, supports and confidence to me during this thesis. Additionaly, I would like too deeply thanks to my grandmother Müzeyyen GEBEDEK who was supported me during my education period in all manners. I also believe that she is still watching me and she is quite proud of my graduation.

At the end, I would like to thank everybody to who helped me to walk this way.

April 2014

Buket ALKAN
Chemist

TABLE OF CONTENTS

Page

ABBREVIATIONS

AFC : Alkaline Fuel Cell
AMPS : 2-Acrylamido-2-metyhlpropan sulfonic acid
ATRP : Atom Transfer Radical Polymerization
Bpy : 2-2'-bipyridine
C/LRP : Controlled/living radical polymerization
DDC : *N*,*N*-Diethyl dithiocarbomate
DMF : Dimethyl formamide
DMFC : Direct methanol fuel cell
DSC : Differential scanning calorimeter
EIS : Electrochemical impedance spectroscopy
FC : Fuel Cell
FRP : Free Radical Polymerization
FT-IR : Fourier transform infrared spectroscopy
GDL : Gas diffusion layer
MCFC : Molten carbonate fuel cell
MEA : Membrane electrode assembly
MeOH : Methanol
NMR : Nuclear magnetic resonance
PAFC : Phosphoric acid fuel cell
PEMFC : Polymer electrolyte membrane fuel cell
PEM : Polymer electrolyte membrane
PFSA : Perfluorosulfonic acid
PMDETA : N,N,N',N'',N″-pentamethyldiethylenetriamine
RAFT : Reversible Addition Fragmentation Chain Transfer
SPMAK : 3-sulfo prophyl methacrylate potassium salt
SOFC : Solid oxide fuel cell
***t*BA** : *tert*-butyl acrylate
TFA : Trifluoroacetic acid
THF : Tetrahydrofuran
T_g : Glass transition temperature

LIST OF TABLES

Page

LIST OF FIGURES

Page

POLYSULFONE-BASED AMPHIPHILIC POLYMERS

SUMMARY

Over the last decade, polymer electrolyte membrane fuel cells (PEMFCs) have received ever growing interest resulting in significant technological progress, especially in areas of increasing power density. The membrane electrode assembly (MEA) which acts as both a separator and an electrolyte in the operating fuel cell, is the key component of PEMFCs to determine the fuel cell performance and its lifetime. The requirements for an excellent membrane are multiply and stringent, including high protonic conductivity, flowreactant gas permeability, thermal, mechanical and chemical stability.

The fluoropolymer (PFSA) Nafion, a DuPont product which shows good thermal stability and high proton conductivity, is the one of the most common and commercially available PEM materials. On the other hand, high methanol permeability, high cost and proton conductivity loss above 100 °C give negative effect to Nafion. Therefore, several studies have been carried out to identify different types of non-fluorinated polymers as alternative to the Nafion® and in some case, comparable performances to the Nafion® in terms of proton conductivity and thermo-chemical properties. Despite polysulfone (PSf) is a popular membrane because of good thermal and chemical stability, mechanical strength and excellent oxidative resistance, the hydrophobic nature of PSf gives some limitation in membrane application. Thus, hydrophilic PSf membrane surfaces have created using a variety of methods.

Here are reported, PSf backbone was functionalized by 2-Acrylamido-2-methylpropan sulfonic acid (AMPS), 3-sulfopropyl methacrylate potassium salt (SPMAK) and *tert*-butyl acrylate (*t*BA) by using iniferter method and atom transfer radical polymerization (ATRP).

First, PSf was functionalized by chloromethylation reaction, also PSf-DDC was synthesized from the reaction of chloromethylated PSf with sodium diethyl dithiocarbomate trihydrate for iniferter method. AMPS as sulfonic acid groups containing monomer were grafted to PSf backbone.

Second, SPMAK and *t*BA were grafted to PSf backbone using chloromethylated PSf as a macroinitiator by ATRP. Then the proton conductivity and thermal stability in grafted polymer have been investigated for PSf based membranes.

POLİSÜLFON ESASLI AMFİFİLİK POLİMERLER

ÖZET

Günümüzde enerji ihtiyacını karşılamak için kullanılan fosil yakıtların sınırlı olması ve bu tür yakıtların yanması ile oluşan ürünlerin çevreye verdiği ciddi zararlar sonucunda yeni ve temiz enerji kaynakların kullanımını zorunlu hale getirmiştir. Fosil yakıtlara alternatif olarak geliştirilecek bir enerji kaynağı özellikle çevreye zarar vermemeli, uygulanabilir ve düşük maliyetli olmalıdır. Bu yöndeki çalışmalar sonucunda ortaya çıkan temiz enerji kaynaklarından birisi de hidrojen enerjisidir. Hidrojenin doğrudan yakıt olarak kullanılmasının yanında hidrojenin ve oksijenin yakıt olarak kullanarak elektrokimyasal tepkime ile elektrik üreten yakıt pillerinin geliştirilmesi üzerine de yoğun bilimsel araştırmalar yapılmaktadır. Modüler olmaları nedeniyle yakıt pillerinin küçük taşınabilir elektronik cihazlardan ulaşım alanındaki uygulamalara kadar potansiyel kullanım sahaları çok geniştir. Elektrolit kullanım tiplerine göre yakıt pilleri birkaç çeşide ayrılabilir, bunlar başlıca bazik, erimiş karbonat, fosforik asit, katı oksit ve proton değişim membranlı (PEM) yakıt pilleridir

PEM yakıt hücrelerinin temel bileşeni anot ve katot olmak üzere iki tane elektrot içerir. Bunlar birbirlerinden polimer membran elektrolit ile ayrılmışlardır. Her iki elektrot bir kenarlarından ince platin katalizör tabakası ile örtülmüştür. Yakıt olarak kullanılan hidrojen yakıt hücresinin anot kenarından beslenir. Anotta platin katalizör varlığında serbest elektronlar ve protonlara ayrışır. Serbest elektronlar dış çevrimde kullanılırlar ve elektrik akımını oluştururlar. Protonlar polimer membran elektroliti geçerek katota doğru hareket ederler, katotta havadan gelen oksijen dış çevrimden gelen elektronlar ve protonlar saf su ve ısı oluşturmak üzere birleşirler. PEM yakıt pili elektrotları üzerinde gerçekleşen reaksiyonlar aşağıdaki gibidir;

$H_2\,(g) \rightarrow 2H^+ + 2e^-$ anot tepkimesi

$2H^+ + 2e^- + 1/2O_2 \rightarrow H_2O$ katot tepkimesi

PEM'lerin çalışma sıcaklığı 80-90 ºC gibi çok düşük sıcaklıklarda ve çalışma basınçları da 1-8 atm basınç arasındadır. Bu tip yakıt hücreleri belli bir nem oranında hidrojen ve oksijen ile çalışabilmektedir.

PEM yakıt hücreleri düşük sıcaklıkta çalışmaları, sessiz olmaları ve yüksek güç yoğunluğuna sahip olmalarından ötürü önemli bir alternatif enerji kaynağıdır. Yüksek güç yoğunluğu için önemli bir faktör olan konu; membran ve elektrot takımı arasındaki su dengesinin iyi yönetilmesidir. Ayrıca PEM yakıt hücrelerinin performansı membranın iletkenliğine bağlıdır. PEM yakıt hücrelerinde su katotta üretilir. En ideal halde bu oluşan su, elektroliti gereken nemlilikte tutar. Katottan verilen hava, reaksiyon için gereken oksijeni karşılamaya ve oluşan fazla suyu uzaklaştırmaya yeterli olur. Katottan anoda suyun difüzyonu sonucu elektrolitin tüm yüzeyi istenilen nemlilikte olur. Bu nedenle katotta üretilen suyun yönetimi oldukça önem kazanır.

Eğer su taşınımı, suyun üretiminden az ise katotta aşırı su birikimi olması sonucunda

su taşmaları oluşarak oksijenin katot katalizör ve gaz difüzyon tabakalarının gözeneklerinden transferi engellenmiş olur. Bu problem yakıt hücresinin performansını düşürür. Su taşınımı su üretiminden fazla ise membranın kuruması söz konusu olur. Bu da membran iletkenliğinin azalmasına, dolayısıyla membranın proton geçirgenliğinin azalmasına neden olur. Katottaki su fazlalığı, orta ve yüksek akım yoğunluklarında işlem parametreleriyle kontrol edilir.

Yüksek güç yoğunluğu, hızlı ve çabuk marş yapabilme ve değişken güç çıkışına uygun olması PEM yakıt pillerinin ulaşım alanında kullanılabilmesini uygun kılmaktadır. Ayrıca PEM yakıt hücreleri, özellikle yüksek performanslı polimelerin bulunmasından sonra, uzay çalışmalarında ve özel askeri sistemlerde uygulanmak üzere geliştirilmiştir.

Proton iletim özelliğine sahip polimerik membran bir PEM yakıt hücresinin en önemli elemanıdır. Günümüzde ticari olarak kullanılan membranların çeşitliliğinin az ve maliyetinin yüksek olmasından dolayı alternatif membranların geliştirilmesi üzerine yapılan çalışmalar ivme kazanmıştır. PEM yakıt hücrelerinde kullanılan membranlar;

- Proton geçirgen özellikte olması,
- Su, yakıt (hidrojen veya metanol), oksijen ve havadaki diğer gazları geçirmemesi
- Mekanik dayanımının yüksek olması,
- Uzun süreli kullanımda ısıl ve kimyasal direnci yüksek,
- Teknolojik olarak yaygın bir şekilde kullanılabilmesi için emniyetli ve ucuz olması

gerekmektedir. Tüm bu özellikleri ek olarak, membran yüksek iyon iletkenliğie ulaşabilmesi için su ile tamamen doyurulmalıdır.

Yakıt hücresindeki polimerik membranın iyon iletkenliğine sahip olmasına rağmen elektronları geçirmez bu nedenle görevi protonu anot bölgesinden katot bölgesine iletmektir. Membran bünyesindeki su molekülleri, proton ile zayıf bağlar oluşturarak hidrojen iyonunun anot bölgesinden katot bölgesine ilerlemesini sağlar. Plakadan geçmeyen elektronlar, harici bir devre yardımıyla hücrenin diğer tarafına (katot) alınır ve devrelerini tamamlarlar.

Termoplastik polimerler sınıfından olan polisülfon (PSf) ısı ve kimyasal dayanımının yüksek olması, mekanik mukavemeti ve oksitlenmeye karşı gösterdiği direnç sayesinde membran uygulamarında ilgi çekmektedir. Fakat polisülfonun hidrofobik doğası membran uygulamalrında bazı kısıtlamalara neden olmaktadır. Bunun üstesinden gelmek için çeşitli yöntemler kullanılarak hidrofilik PSf membran yüzeyi oluşturulmaktadır.

Bu çalışmada ana zincir olarak PSf kullanılıp, bu polimere hidrofilik karakter kazandırmak için çeşitli monomerler (AMPS, SPMAK ve *t*BA) aşı kopolimerizasyonu ile bağlanmıştır. Bu polimerlerin sentezlenmesi için iki farklı polimerizasyon çeşidi kullanılmıştır. Bunlar ATRP ve iniferter polimerizasyon metotlarıdır.

ATRP çok yönlü kontrollü radikal polimerizasyon metotlarından biridir. Bir ATRP sistemi; başlatıcı, metal halojenür, ligand ve monomerden oluşmaktadır. Düşük oksidasyon basamağına sahip metal kompleksi (M_t^n compleks/Ligand), radikal ve

daha yüksek oksidasyon basamağına sahip metal kompleksi (X-M_t^{n+1}/Ligand) üretmek üzere alkil halojenür (R-X) ile reaksiyona girer. Oluşan radikal monomere eklenir ve böylece polimer zincirinde büyüme gerçekleşir. Reaksiyonun ilerleme aşaması halojenürün koparılması sonucu oluşan serbest radikal üzerinden ilerler. Serbest radikal metalden halojenürü tekrar koparır ve aktif olmayan ürün oluşur. Bu işlemler oldukça hızlıdır ve reaksiyonda denge aktif olmayan ürün oluşumu yönündedir. Aktivasyon ve deaktivasyon hız sabitlerinin oranına bağlı olarak bir süre sonra büyüyen zincir yine aktif hale gelir ve büyümeye devam eder. Bu basamaklar tekrarlanarak kontrollü zincir büyümesi sağlanmış olur. Sonlanma tamamen önlenemez, ancak sonlanan zincirlerin oranı büyüyen zincirlerle karşılaştırıldığında sonlanan zincirlerin sayısı oldukça küçüktür.

ATRP reaksiyonu ortamdaki monomer bitene kadar ya da reaksiyon koşulları bozulana kadar devam eden bir yaşayan polimerleşme tekniğidir. İstenilen ağırlıkta polimer elde edene kadar reaksiyon devam edebilir ve reaksiyonu durdurmak için dışarıdan müdahale gerekmektedir.

Bu çalışmanın ATRP basamağında, PSf ilk önce klorometilleme reaksiyonu ile fonsiyonlandırılmış ve elde edilen polimer makro başlatıcı olarak kullanılarak SPMAK ve *t*BA monomerleri ATRP koşulları altında PSf ana zincirine aşı yöntemiyle bağlanmıştır.

Diğer yöntem olan iniferter polimerizasyonu ise bir iniferter grubun ışık veya ısı ile radikal üretmesi ve monomerin başlatıcı radikali ile kontrollü mekanizmayı sağlayan sonlandırıcı radikal grubunun arasına dolması ile gerçekleşir. Bu çalışmada iniferter grup olarak, sodyum dietilditiyokarbomat kullanılmıştır. Makrobaşlatıcı olarak önce klorometillenmiş PSf ile sodyum dietil ditiyokarbomat reaksiyona sokulmuş ve PSf-DDC makrobaşlatıcısı sentezlenmiştir. Ardından ışık ile PSf üzerinde bulunan DDC gruplarından AMPS monomerinin katılması iniferter polimerizasyonu gerçekleştirilmiş.

İki farklı metotla sentezlenen aşı kopolimeri FT-IR, ^{1}H NMR ile karakterize adilmiş termal özellikleri DSC ölçümleri ile belirlenmiştir.

Çalışmanın amacına uygun olarak sentezlenen maddelerin iyon iletkenlikleri Elektrokimyasal Empedans Spektrometresi (EIS) ile incelenmiştir.

1. INTRODUCTION

Energy consumption which is heavily dependent on burning fossil fuels acts an important part in our daily life. The increasing concentration of carbon dioxide (CO_2) in the atmosphere due to fossil fuel depletion is a key cause of global warming which reduces agricultural production and causes other biological and social problems. To overcome this negative effects of fossil fuels, regenerative energy sources, such as solar, wind, geothermal and hydroelectric energies are sought. An alternative way to save valuable natural resources and solve the environmental problem is to develop cleaner and more efficient energy conversion devices [1, 2].

Hydrogen which can be made from water by electrloysis,using any source of dc electricity, is seen as one of the most promising candidates of these alternate energy resources for being the lightest, cleanest and most efficient fuel. The gas can be stored, distributed and burnt to release heat. In addition hydrogen is not cause pollution due to the fact that water is the only product of combustion [3]. The most important property of hydrogen energy is its direct conversion into electricity in fuel cells with higher efficiencies than conversion of fossil fuels in traditional combustion engines or to electrical energy in thermal power plants. Therefore, in recent years, fuel cell research and development have received much attention for its higher energy conversion efficiency and lower or non greenhouse-gas emissions than thermal engines in the processes of converting fuel into usable energies.

Fuel cell is a device that converts the chemical energy from a fuel into electricity through a chemical reaction with oxygen or another oxidizing agent. Hydrogen is the most common fuel, but hydrocarbons such as natural gas and alcohols like methanol are sometimes used. Fuel cells are often compared to batteries. Both convert the energy produced by a chemical reaction into usable electric power. However, the fuel cell will produce electricity as long as fuel (hydrogen) is supplied, never losing its charge.

Fuel cells come in many varieties, however, they all work in the same general manner. They are made up of three adjacent segments; the anode, the electrolyte, and the cathode. Two chemical reactions occur at the interfaces of the three different segments. The net result of the two reactions is that fuel is consumed, water or carbon dioxide is created, and an electric current is created, which can be used to power electrical devices. There are five families of fuel cells (FC). These are phosphoric acid fuel cells, proton exchange membrane (PEM) fuel cells, alkaline fuel cells, molten carbonate fuel cells, and solid oxide fuel cells; each have their own advantages and disadvantages. Significant progress has been made with hydrogen PEM fuel cells in the last decade. This thesis research will focus on polymer electrolyte membrane fuel cells (PEMFC).

Proton-exchange membrane fuel cells (PEMFCs) are considered to be a promising technology for clean and efficient power generation in the twenty-first century. One current thrust of fuel cell research is to increase the operating temperature of PEM fuel cells to 120ºC or above. The operation of the polymer electrolyte membrane fuel cell (PEMFC) at high temperatures (>120 ^{o}C, preferably > 150 ^{o}C) is desirable because of the enhanced catalyst activity, reduced poisoning effect of fuel impurities, simplification of the system, and easy thermal compatibility [4]. To be used commercially, fuel cells must meet criteria including fast startup, high power density, high fuel efficiency, easy and safe handling, long life-span and low cost. None of the cell types yet satisfy all these requirements.

The membrane electrode assembly (MEA) is at the heart of the single cell. It is the critical component of the PEMFC, since it is the site of the fuel cell reactions. The MEA, is less than a millimetre thick and consists of a solid polymer, proton conducting membrane electrolyte, with a layer of platinum-based catalyst and a gas-porous electrode support material on both sides of it, forming the anode and cathode of the cell. One of the most common and commercially available PEM materials is the fluoropolymer (PFSA) Nafion, a DuPont product. While Nafion is an ionomer with a perfluorinated backbone like Teflon, there are many other structural motifs used to make ionomers for proton exchange membranes. Many use polyaromatic polymers while others use partially fluorinated polymers [5].

Nafion® is based on sulfonated fluorocarbon polymer and shows good thermal stability and high proton conductivity as advantages, while high methanol

permeability (methanol crossover), high cost (about 900-1000 US $/m^2) and proton conductivity loss above 100 °C represent the disadvantages. Therefore, several studies have been carried out to identify different types of non-fluorinated polymers as alternative to the Nafion® and and in some case, comparable performances to the Nafion® in terms of proton conductivity and thermo-chemical properties, as well as lower crossover and costs [2].

Despite polysulfone (PSf) is a popular membrane because of good thermal and chemical stability, mechanical strenght and excellent oxidative resistance, the hydrophobic nature of PSf gives some limitation in membrane application. Thus, hydrophilic PSf membrane surfaces have created using a variety of methods and chemical reaction of hydrophilic components onto the membrane surface or bulk PSf [6, 7] is one of these method. Atom transfer radical polymerization (ATRP) is one of the controlled free radical polymerization techniques. ATRP is one of the most versatile methods for synthesizing homopolymers and copolymers with predetermined molecular weights and narrow molecular weight distributions. It is based on the combination of an organic halide initiator (RX) with a metal/ligand catalytic system, which is able to promote fast initiation compared to propagation and then reversibly activate halogenated chain, ends (P*n*X) during polymerization.

Photopolymerization has some advantages over thermally initiated polymerization. This is evidence in the rapid growth of radiation curing as an industrial process, which depends on the use of photoinitiators. Photoinitiators can be used in controlled radical reactions. The use of N,N-diethyl dithiocarbamate (DDC) derivatives as so-called photoiniferters during radical polymerization reactions has been reported. The term iniferter is used as first coined by Otsu, meaning substances that act as initiator, transfer agent and terminator in radical polymerization reactions [8].

In this study, PSf backbone was functionalized with 2-Acrylamido-2-methylpropan sulfonic acid (AMPS) by using iniferter method, 3-sulfopropyl methacrylate potassium salt (SPMAK) and *tert*-butyl acrylate (*t*-BA) by using ATRP, also.

First, PSf was functionalized by chloromethylation reaction, also PSf-DDC was synthesized from the reaction of chloromethylated PSf with sodium diethyl dithiocarbomate trihydrate for iniferter method. AMPS as sulfonic acid groups containing monomer were grafted to PSf backbone by using PSf-DDC.

Second, SPMAK and *t*BA were grafted to PSf backbone using chloromethylated PSf as a macroinitiator by ATRP. Then the proton conductivity and thermal stability in grafted polymer have been investigated for PSf based membranes.

2. THEORETICAL PART

2.1 Fuel Cells

The fuel cells are electrochemical energy conversion devices that convert the chemicals hydrogen and oxygen into water and in the process produces electricity.

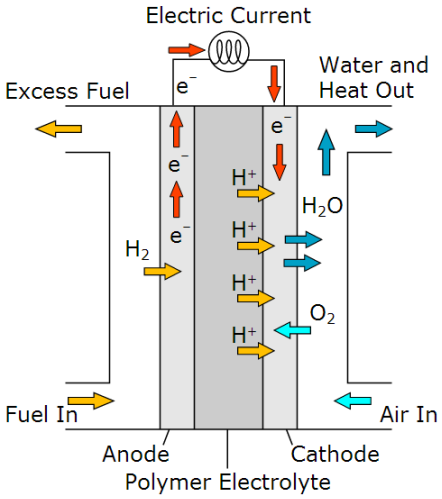

Figure 2.1 : Schematic of PEM fuel cell.

It produces electricity from external supplies of fuel (on the anode side) and oxidant (on the cathode side). These react in the presence of an electrolyte. Generally, the reactants flow in and reaction products flow out while the electrolyte remains in the cell. Fuel cells can operate virtually continuously as long as the necessary flows are maintained as seen in Figure 2.1. Current methods for the conversion of chemical energy to electrical energy are rather inadequate and wasteful. The fuel cell has a high-energy conversion efficiency of more than 40–50% that is higher than a coal fired power station or an internal combustion engine. It has no moving parts apart from the air and fuel blowers and is therefore more reliable and less noisy, has a lower maintenance cost and a long operating life compared to an equivalent coal-fired power station or internal combustion engine. Additionally, it is the clean energy without any harmful emission to the environment [9].

Fuel cells are very useful as power sources in remote locations such as spacecraft, remote weather stations, large parks, rural locations, transport, mobile and stationary sector and in certain military applications [10-14].

2.1.1 Historical developmet of fuel cell

The first working fuel cell was invented by Sir William Grove in 1843 which produced water and electricity by reacting oxygen and hydrogen on separate platinum electrodes that were immersed in dilute sulfuric acid inside. Unfortunately, there were no practical fuel cells developed for the following 100 years. In the 1920s, early German fuel cell research developed primitive carbonate and solid oxide fuel cells. One of the most important milestones in fuel cell history is an invention of polymer electrolyte membrane (PEM) in 1955 when Willard Thomas Grubb in General Electric (GE) modified the original fuel cell design with a sulfonated polystyrene ion-exchange membrane as the electrolyte. In 1959, Francis T. Bacon developed a 5kW fuel cell that used alkaline electrolyte and nickel electrodes [11]. A more efficient design of the fuel cell was made in the 1960s for the Gemini and Apollo space missions that fuel cell technology came of age. General Electric (GE) produced the fuel cell powered electrical power system for NASA's Gemini and Apollo space capsules that also provides drinking water for the crew. Better polymer electrolyte material, sulfonated tetrafluorethylene copolymer (Nafion®), was discovered in late 1960s by Walther Grot at DuPont. With its excellent thermal and mechanic stability, Nafion® became the most widely used electrolyte material for PEM fuel cells [15]. The use of solid polymer electrolyte membrane has established the base for the modern fuel cell technology because the fuel cell with polymer electrolyte membrane is much simpler and more reliable than that of using liquid electrolyte. The second important factor in fuel cell history is the development of electrode catalysts for oxygen reduction and fuel oxidation. Much effort has been made to seek non-platinum catalysts, such as metalloporphyrins and metallo-phthalocyanines for catalytic oxygen reduction. Up to the present, electrode catalysts and electrolyte membranes are still the major challenges in fuel cell research and development.

2.1.2 Fuel cell systems

For practical application, a number of single fuel cells connected in series form a fuel cell stack to gain higher voltage and power including fuel cell stacks, pumps, batteries, sensors, fuel cartridge and electronic controller.

In the following pages, a brief overview of the basic electrochemical processes in a H_2/O_2 PEM fuel cell is given, followed by information on individual fuel cell components: anode, cathode, catalyst support, membrane, gas diffusion layers, and bipolar plates [16]. It has been seen that many chemical reactions can be regarded as the transfer of electrically charged electrons from one atom to another. Such a transfer can be arranged to occur through a wire connected to an electrode in contact with atoms that either gain or lose electrons. In that way, electricity can be used to bring about chemical reactions, or chemical reactions can be used to generate electricity [17].

For economic reasons, air is usually used as the cathode feed rather than pure O_2. Electrons are carried from the anode to the cathode through the external electric circuit. The anode and cathode electrode layers are typically made of Pt or Pt alloys dispersed on a carbon support for maximum catalyst utilization. Ionomers and polytetrafluoroethylene (PTFE) resins can be added to the electrode layers.

GDLs are made of porous media such as carbon paper or carbon cloth to facilitate the transport of gaseous reactants to the electrode layers, as well as the transport of electrons and water away from the electrode layers. An MEA is sandwiched between two bipolar plates to form a single fuel cell [18]. The word *bipolar* refers to a plate's bipolar nature in a series of single cells (known as a stack) in which a plate (or a set of half plates) is anodic on one side and cathodic on the other side.

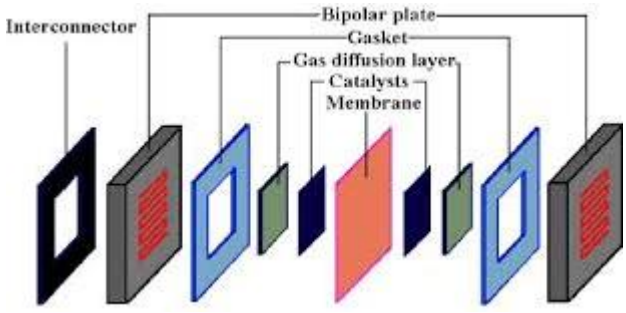

Figure 2.2 : Schematic views of a PEM fuel cell and a seven-layered MEA.

Figure 2.2 is a schematic view of a typical PEM fuel cell components [16]. A MEA usually refers to a five-layer structure that includes an anode GDL, an anode electrode layer, a membrane electrolyte, a cathode electrode layer, and a cathode GDL. Most recently, several MEA manufacturers started to include a set of membrane sub gaskets as a part of their MEA packages. This is often referred to as a seven-layer MEA. In addition to acting as a gas and electron barrier, a membrane electrolyte transports protons (H^+) from the anode, where H_2 is oxidized to produce H^+ ions and electrons, to the cathode, where H^+ ions and electrons recombine with O_2 to produce H_2O [16].

2.1.3 Types of fuel cell

The fuel cells may be classified based on the type of electrolyte used. This classification determines the kind of chemical reactions that take place in the cell, the kind of catalysts required, the temperature range in which the cell operates, the fuel required, and other factors. These characteristics, in turn, affect the applications for which these cells are found most suitable. There are several types of fuel cells currently under development, each with its own advantages, limitations, and potentialapplications. According to the characteristics of the electrolytes, they are divided into roughly five types: alkaline (AFC), phosphoric (PAFC), molten carbonate (MCFC), solid oxide (SOFC), and polymer electrolyte (PEFC) [19]. Much attention has been devoted to PEFC including direct methanol fuel cell (DMFC) recently. The features of such fuel cells are listed in Table 2.2.

Table 2.1 : Fuel cell types and their main characteristic.

Fuel Cell Type	Electrolyte	Operating Temperature	Efficiency	Electrical Power	Possible Application
AFC	Potassium hydroxide	60-90 °C	45-60%	Up to 20 kW	Submarines Spaceships
MCFC	Immobilized liquid molten carbonate	650 °C	45-60%	>1 mW	Power stations
PAFC	Immobilized liquid phosphoric acid	200 °C	35-40%	>50 kW	Power stations
PEMFC	Ion exchange membrane	80 °C	40-60%	Up to 250 kW	Vehicles
SOFC	Ceramic	1000 °C	50-60%	>200 kW	Power stations

Among all kinds of fuel cells, proton exchange membrane (PEM) fuel cells are compact and lightweight, work at low temperatures with a high output power density and low environmental impact, and offer superior system startup and shutdown performance. These advantages have sparked development efforts in various quarters of industry to open up new field of applications for PEM fuel cells, including transportation power supplies, compact cogeneration stationary power supplies, portable power supplies, and emergency and disaster backup power supplies.

2.1.4 Application of fuel cell

Nowadays, fuel cell categorises the use of fuel cells into three broad areas, defined as portable, stationary and transport. Portable fuel cells encompass those designed to be moved, including auxiliary power units (APU), stationary power fuel cells are units designed to provide power to a fixed location and transport fuel cells provide either primary propulsion or range-extending capability for vehicles. The only practical application of low temperature fuel cells considered in this chapter are AFCs in the American space shuttles. On the other hand, PAFCs have been used in stationary power generation plants since the 70s. Finally, PEFCs have experimented a resurgence in the 90s due to their performance improvement, as a consequence of the use of a new proton exchange membrane (Nafion®) and new techniques that enhanced the efficiency of platinum catalyst in the electrodes. This resurgence has been mainly directed towards portable and transport applications rather than stationary applications.

Horizon Fuel Cell Technologies is one of the largest suppliers of these systems and has improved its offering over the years, producing more and more advanced products. Its latest fuel cell powered remote control car is designed to be controlled by a smartphone, with the standard controls replaced by an app where users can control the car by tilting their phone. The car comes with its own refuelling station, which can be powered either by a solar panel or through a USB connection, thereby avoiding the perennial 'chicken-and-egg' problem.

Military organisations around the world continue to show interest in fuel cell technology, evaluating it as a means to significantly reduce the weight carried by soldiers in the field. FC used in military is designed to be vehicle-mounted to provide power for communications, night vision, navigation and any additional requirements.

Industrial vehicles powered by 10 kW to 50 kW PEM fuel cells. These vehicles include forklifts and people movers. Hydrogen is the fuel of choice for these applications. Automotive PEM fuel cells with PEM systems power ratings from 50 kW to 100 kW. PEM systems with power ratings from 100 kW to 300 kW for heavy-duty vehicles such as buses. Hydrogen is the fuel of choice for these applications [20].

Recently a number of venture corporations put small fuel cells for stationary use out to the public. These applications involve generation of both power and heat, and can range from home units (output starting at 2 kW) to block-type units that supply entire residential areas (with outputs in the MW range). Conventional block-type or block-unit power stations use combustion engines and gas turbines to generate both electricity and heat. A new type of these power plants could instead be powered by fuel cells. The advantages of this technology include high efficiency as well as a drastic reduction in emissions and noise pollution.

HydroGen3, a fuel cell car developed by Adam Opel AG, is propelled by a fuel cell stack consisting of 200 individual PEM fuel cells connected in series. The fuel cells produce energy without noise and, since there are no moving parts involved, also without wear and tear. The HydroGen3's stack has a maximum output of 129 kW. The motor's maximum power is 60 kW. Its efficient propulsion allows this fuel cell car to accelerate from 0 to 100 km/h in approximately 16 seconds and attain maximum speeds of around 150 km/h [21].

Most big motor companies such as Toyota, Honda, Nissan, GM, Ford, Daimler Chrysler, Hyundai and Volkswagen joined the California Fuel Cell Partnership car rally that started in 1999 and ended its phase I in 2003. Phase II started in 2004 and will last until 2007. They have tested the fuel cell operation on board and the hydrogen stand and other subsidiary appliances.

The Japanese government bought several fuel cell cars in 2002 and is now using them for commuting purposes in the inner-city area. These are the first commercialized cars of this sort in the world [22].

2.2 Polymer Electrolyte Membrane Fuel Cell

Proton exchange membrane fuel cells (PEMFC) are among the most promising electrochemical devices for convenient and efficient power generation. The proton exchange membrane (PEM) is a key component in the system, which functions as an electrolyte for transferring protons from the anode to the cathode as well as providing a barrier to the passage of electrons and gas cross-leaks between the electrodes [11]. The membrane is very small and light and in order to catalyse the reaction, platinum catalyst is used on either side of the membrane.

PEMFC needs only hydrogen, oxygen from the air, and water to operate and does not require corrosive fluids like some other fuel cells typically fuelled with pure hydrogen supplied from storage tanks or on-board reformers. Reactants enter the cell through gas channels, which are embedded in the current collectors (bipolar plate). GDLs are used to uniformly distribute the reactants across the surface of the catalyst layers (CL), as well as to provide an electrical connection between the catalyst layers and the current collectors.

Within the PEM fuel cell unit, hydrogen molecules at the anode split into protons and electrons. The protons pass across the polymeric membrane to the cathode while the electrons are pushed round an external circuit to produce electricity. Oxygen (in the form of air) is supplied to the cathode and this combines with the hydrogen ions to produce water. The relatively low temperature of operation (about $80^{o}C$) allows for the system to start quickly (less warm-up time) and results in less wear on components, resulting in better durability.

On the anode surface, hydrogen is oxidized to proton and the proton migrates to the cathode surface through the electrolyte membrane. On the cathode, oxygen is reduced in the presence of proton to water.

$$\text{At the anode:} \quad H_2 \longrightarrow 2H^+ + 2e^-$$

$$\text{At the cathode:} \quad 2H^+ + 1/2O_2 + 2e^- \longrightarrow H_2O\ (l)$$

$$\text{Total reaction:} \quad H_2 + 1/2O_2 \longrightarrow H_2O\ (l)$$

2.2.1 Commercial proton exchange membran for fuel cell

2.2.1.1 General

One of the most important components in a proton exchange membrane fuel cell is the actual proton exchange membrane (PEM). The proton exchange membrane performs two basic, essential functions in PEMFCs, one of this is a separator to prevent mixing of the fuel (i.e., hydrogen gas, methanol, etc.) and the oxidant (i.e., pure oxygen or air), and the another one is an electrolyte for transporting protons from the anode to the cathode. In order to meet the cost and durability target, a membrane electrolyte must meet several functional requirements [23]:

- high proton conductivity over a wide RH range
- low electrical conductivity
- low gas permeability, particularly for H_2 and O_2 (to minimize H_2/O_2 crossover)
- good mechanical properties under cycles of humidity and temperature
- stable chemical properties
- quick start-up capability even at subzero temperatures
- low cost

The lifetime of a membrane is related to its original thickness, its mechanical integrity, and the chemical stability of the constituent ionomers. There are many factors that can affect the membrane lifetime. These include not only the membrane properties (such as its chemical structure, composition, morphology, configuration, and fabrication process), but also several external factors (such as contamination of the membrane, materials compatibility, and the operating conditions of the fuel cell).

2.2.1.2 Types of proton exchange membrane

The first employed proton exchange membrane fuel cell in the Gemini program was a crosslinked polystyrene sulfonic acid (PSSA) [23]. The one-kilowatt (1 kW) fuel cell stack was used as both an auxiliarypower source and as a source of water for the astronauts. However, the polystyrene sulfonic acid was not durable under the actual PEMFC operation conditions. One modern method for innovating some novel copolymers has been to induce grafting and/or crosslinking. Grafting sulfonate-containing moieties is rationalized to force phase separation of the sulfonic acids

generating ion-conducting domains [24]. As extensively reported in the literature, styrenic monomers are widely available and easy to modify, and their polymers are easily synthesized via conventional free radical and other polymerization techniques. Presently, two commercial (or semicommercial) PEMs are based on styrene or styrene-like monomers: BAM from Ballard, and Dais Analytic's sulfonated styrene-ethylene-butylene-styrene (SEBS) membrane. The stability of these aliphatic hydrocarbon copolymers is, in general, inferior to the current state-of-the-art perfluorinated copolymers [24]. For this reason, the Dais membranes are being promoted for the low temperature (<60 ^{o}C), portable power markets.

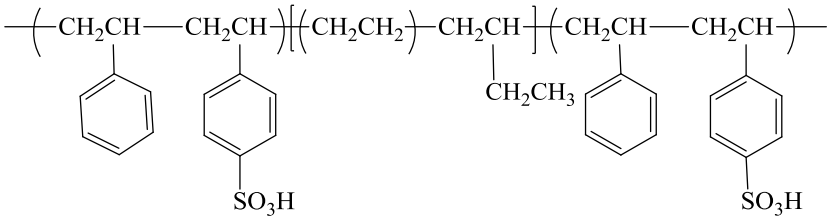

Figure 2.3 : Structure of Dais Analytic's triblock PEM [25].

PEM fuel cells, the commercially mature membrane is a perfluorosulfonic acid (PFSA) membrane, such as Nafion® (DuPont), Aciplex® (Asahi Chemical), and Flemion® (Asahi Glass), which have a similar structure and conduct protons via sulfonic acid groups (-SO_3H). Nafion's poly(perfluorosulfonic acid) structure imparts exceptional oxidative and chemical stability, which is also important in fuel cell applications.

The rate of PFSA degradation depends strongly on fuel cell operating conditions such as RH, temperature, H_2/O_2 crossover rate, CO concentration, air bleed level, and electrode potential. Peroxide radicals from decomposition of H_2O_2 are believed to be responsible for membrane chemical degradation. The generally accepted end-group degradation mechanism, the so-called unzipping mechanism, starts from the end groups of a perfluorinated polymer chain.

Wholly aromatic polymers are thought to be one of the more promising routes to high performance PEMs because of their availability, processability, wide variety of chemical compositions, and anticipated stability in the fuel cell environment. Specifically, poly(arylene ether) materials such as poly-(arylene ether ether ketone) (PEEK), poly(arylene ether sulfone), and their derivatives are the focus of many investigations, and the synthesis of these materials has been widely reported.

2.2.1.3 Nafion®

A perfluorinated polymer with pendant sulfonated side chains, Nafion® was initially developed in 1968 by Walther G. Grot of DuPont for the chlor-alkali cell project of the National Aeronautics and Space Administration (NASA) space program.

Nafion® is the most commonly used and investigated PEM in fuel cells. The electrolyte consists of an acidic polymeric membrane that conducts protons but repels electrons, which have to travel through the outer circuit providing the electric work. A common electrolyte material is Nafion® from DuPont™, which is a free radical initiated copolymer of a crystallizable hydrophobic tetrafluoroethylene (TFE) backbone sequence with a comonomer which ultimately has pendant side chains of perfluorinated vinyl ethers terminated by perfluorosulfonic acid groups. The reported chemical structure of Nafion for PEM membranes is shown in Figure 2.3. Alternatively, the term "equivalent weight" is used to express the mass of electrolyte per unit charge and this equivalent weight provides high protonic conductivity and moderate swelling in water. Nafion has been commercially available in Nafion 117, 115, 112 and 212 films. For Nafion 117, "117" refers to a film having 1100 equivalent weight and a nominal thickness of 0.007 in.

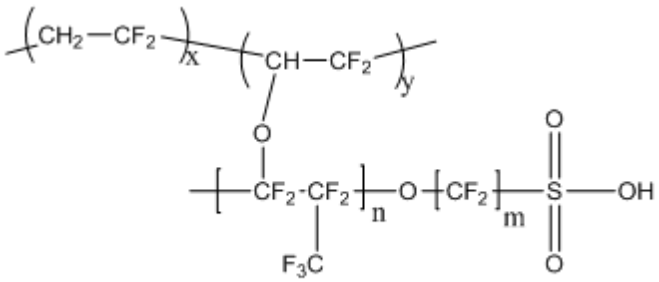

Figure 2.4 : Chemical structure of Nafion® (DuPont).

A perfluorosulfonic polymer such as Nafion® naturally combines, in one macromolecule, the extremely high hydrophobicity of the perfluorinated backbone with the extremely high hydrophilicity of the sulfonic acid functional groups. Especially in the presence of water, this gives rise to a hydrophobic/hydrophilic regions' separation. The sulfonic acid functional groups aggregate to form a well connected hydrophilic domain, which is responsible for the protons and water transport. Vice versa, the hydrophobic domain provides the polymer with the morphological stability and prevents the polymer dissolving in water.

2.2.2 Mechanism of proton conductivity

In PEM fuel cells, proton conductivity relies heavily on the concentration of ion conducting units (most commonly sulfonic acid) in the polymer membrane. While it is desirable to maximize the conductivity of the membrane by increasing its ion content (decreasing equivalent weight), other physical properties must be considered. This type of membrane requires water to conduct protons. The process for proton transport in water is explained by “Grotthuss mechanism" [26]. It is also called “hopping mechanism” or “chain mechanism” or “structure diffusion”. The proton transport comprises rapid intermolecular proton transfers (Hopping) down a chain of hydrogen bonds where the transfer events are assumed to be highly correlated, and reorientation of water dipoles in order to produce a configuration which allows for the next hopping event [26].

However, Nafion requires a minimum of 2-3 molecules of water per sulfonic acid group for dissociation; increasing the water content beyond this increases the hydration and proton mobility is enhanced. In the fully swollen state, after immersion in boiling water, the membrane is plasticized and proton conduction is at its most rapid [18]. At high temperatures and low relative humidity, the water content of the membrane drops and conduction becomes more challenging. One way of reducing the reliance on water would be to increase the acidity of the sulfonic acid group and thus facilitate dissociation. Perfluorinated sulfonated polymers, however, are already highly acidic and increasing the acidity further would be difficult. Sulfonimides alone have been claimed to possess higher acidity than the CF_3SO_3H groups present in Nafion type materials.

Another way to increase proton conduction at low water contents is to reduce the distance between sulfonic acid groups, enabling easier transport. This could be accomplished by increasing the concentration of sulfonic acid groups in the membrane. This approach is limited by the requirement of the membrane to remain insoluble. However, the most advanced commercial membranes do have higher sulfonate concentrations (lower equivalent weights) than the well established Nafion 1100 ionomer.

2.2.3 Water transport within an operating MEA

Water transport to, through and from the membrane involves a complex interplay of processes, as illustrated in Figure 2.5. Included in these processes are the rates of transport of water from the anode to the cathode by electro-osmotic drag (J_{EOD}), and the generation of water at the cathode as the product of the oxygen reduction reaction at a rate (J_{ORR}) that increases with the current density. To ensure the most even water distribution, a membrane enabling rapid water back diffusion from cathode to anode is therefore essential.

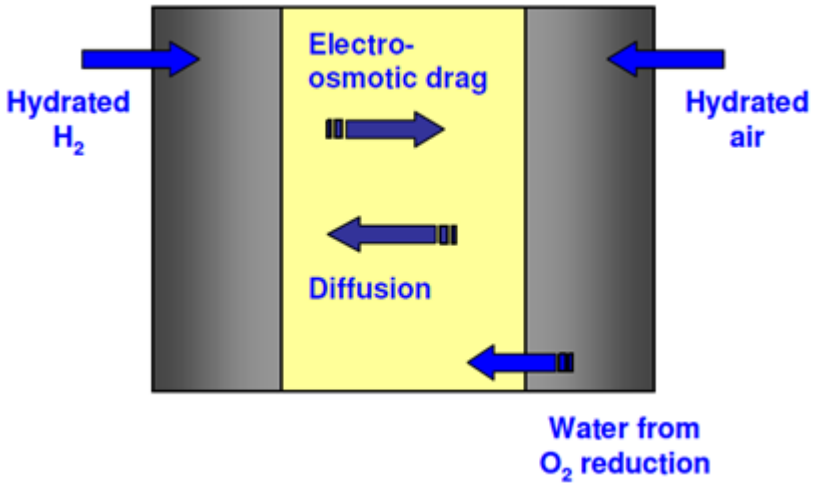

Figure 2.5 : Water management.

2.3 Living Polymerization

Well-defined polymers, with molecular weight, structural and compositional homogeneity, can only be synthesized by living ionic polymerizations or C/LRP methods. The way to living polymerization was opened in 1955 when the seminal work of Szwarc proved that anionic polymerization of poly(styrene) (PS) had truly living character using sodium naphthanelenide initiating system in tetrahydrofuran (THF) [27]. A living polymerization is defined as a chain polymerization without chain transfer and chain termination as indicated by Szwarc. These chain breaking processes were avoided with the development of special high vacuum techniques to minimize traces (<1 ppm) of moisture and air in the anionic polymerization of non-polar vinyl monomers [27]. The synthesis of such copolymers by living anionic polymerization demands fast initiation and relatively slow propagation in order that the distribution of block lengths be controlled. These requirements can be achieved with the use of alkyl lithium initiators in non-polar solvents via the formation of ion

pairs or their aggregates. The ion pairs can essentially be considered dormant species as they have reactivities several orders of magnitude smaller than those of free ions [28]. Exchange processes between dormant and active species are fast enough in comparison with propagation to ensure the production of materials with low polydispersity [29].

After the discovery of living anionic polymerization, critical research on cationic polymerization was performed in the "living" area**.** An equimolar mixture of HI/I_2 was the first system used for the initiation of such polymerizations of vinyl ethers [30]**.** In this system, the initially formed adduct of HI to a vinyl ether is activated by iodine. The fast initiation realized ideal living cationic polymerization of alkyl vinyl ethers. Thus, homopolymers and block copolymers with narrow molecular weight distributions were first synthesized in cationic polymerization.

Undoubtedly, the ionic polymerizations have met several requirements of living polymerization in order to obtain well-defined polymers with controlled chain end functionalities and with well-defined polymer architectures. However, these polymerizations have to be carried out with nearly complete exlusion of moisture and often at low temperatures. Morover only a limited number of monomers can be used, and the presence of functionalities in the monomers can cause undesirable side reactions.

2.4 Controlled / Living Radical Polymerization (C/LRP)

Conventional free-radical polymerization (FRP) techniques are very convenient commercial process for the synthesis of high molecular weight polymers since it can be employed for the polymerization of numerous vinyl monomers under mild reaction conditions, requiring an oxygen free medium, but tolerant to water, and can be conducted over a large temperature range (-80 to 250^{o}C). Furthermore, a wide range of monomers can easily be copolymerized through a radical route, and this leads to an infinite number of copolymers with properties dependent on the proportion of the incorporated comonomers. Moreover, the polymerization does not require rigorous process conditions. The major drawbacks of conventional radical polymerizations are related to the lack of control over the polymer structure. Due to the slow initiation, fast propagation and subsequent irreversible transfer or

irreversible termination, polymers with high molecular weights and high polydispersities are generally produced.

In order to overcome the disadvantages of FRP without sacrificing the above-mentioned advantages, it was recognized that a living character had to be realized in conjunction with the free radical mechanism. Obviously, living polymerization is an essential technique for synthesizing polymers with controlled structures. Moreover, living polymerization techniques allow preparation of macromonomers, macroinitiators, functional polymers, block and graft copolymers, and star polymers.

A truly controlled/living radical polymerization has not been developed until a little more than a decade ago. In the past decade, a number of controlled/living radical polymerization methods have been developed and the three most promising types are: atom transfer radical polymerization (ATRP) (also known as transition metal catalyzed radical polymerization), stable freeradical polymerization (SFRP) (also known as nitroxide-mediated polymerization, NMP), and reversible addition-fragmentation chain transfer (RAFT) polymerization.

2.4.1 Atom transfer radical polymerization (ATRP)

Metal-catalyzed C/LRP, mediated by Cu, Ru, Ni, and Fe metal complexes, is one of the most efficient methods to produce polymers in the field of C/LRP [31]. Among aforementioned systems, copper-catalyzed LRP in conjunction with organic halide initiator and amine ligand, often called atom transfer radical polymerization (ATRP), received more interest. The name atom transfer radical polymerization comes from the atom transfer step, which is the key elementary reaction responsible for the uniform growth of the polymeric chains.

Until the discovery of ATRP, polymer chemists were severely limited in their ability to control the composition and architecture of macromolecules, making it difficult to provide materials with highly specific, uniform characteristics. Since the mid-1950s, many chemists attempted to develop a “living” or controlled polymerization process that would create well-defined polymers in a simple, inexpensive manner. In the mid-1990s, several laboratories across the world surmounted this vexing problem by developing CRP methods. These techniques allow synthesis of fundamentally new materials with complex, well-defined nanoscale architectures. In 1995, Carnegie

Mellon University Professor Krzysztof Matyjaszewski discovered one of the first and most robust CRP methods, ATRP.

ATRP technology developed by Matyjaszewski has already been licensed to nine international companies, which started production of ATRP-based polymers in Japan, Europe and the United States in 2004. ATRP has been successfully used to create better pigment dispersants for inkjet printing, cosmetics, chromatographic packings, adhesives and sealants for self-cleaning windows, among others. Some other applications that are being evaluated include drug delivery methods, coatings for cardiovascular stents, scaffoldings for bone regeneration, biocidal surfaces, degradable plastics and others in the optoelectronic and automotive industries [32].

2.4.1.1 Kinetics and mechanism of ATRP

ATRP, which is the most versatile method of the controlled radical polymerization system, uses a wide variety of monomers, catalysts, solvents, and reaction temperature. ATRP was developed by designing a proper catalyst (transition metal compound and ligands), using an initiator with an appropriate structure, and adjusting the polymerization conditions, such that the molecular weights increased linearly with conversion and the polydispersities were typical of a living process [33]. This allowed an unprecedented control over the chain topology (star, graf, branched), the composition (block, gradient, alternating, statistical), and the end functionality for a large range of radically polymerizable monomers [34-36].

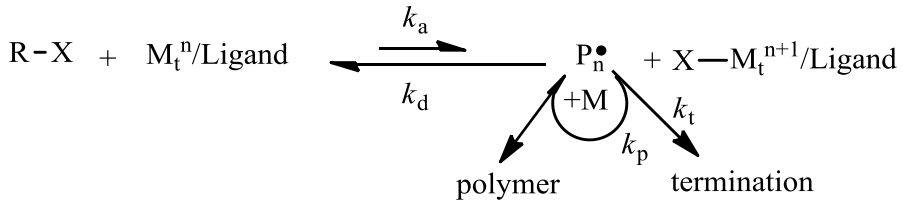

Figure 2.6 : Mechanism of ATRP.

Figure 2.6 represents the general mechanism of ATRP. The radicals, i.e. the propagating species P_n*, are generated through a reversible redox process catalyzed by a transition metal complex (activator, M_t^n–Y/ligand, where Y may be another ligand or a counterion) which undergoes a one-electron oxidation with concomitant abstraction of a (pseudo) halogen atom, X, from a dormant species, P_n–X. Radicals react reversibly with the oxidized metal complexes, X–M_t^{n+} /ligand, the deactivator, to reform the dormant species and the activator. These processes are rapid, and the

dynamic equilibrium that is established favors the dormant species. By this way, all chains can begin growth at the same time, and the concentration of the free radicals is quite low, resulting in reduced amount of irreversible radical-radical termination. Also chain growth occurs with a rate constant of activation, k_a, and deactivation k_d, respectively. Polymer chains grow by the addition of the free radicals to monomers in a manner similar to a conventional radical polymerization, with the rate constant of propagation, k_p. Termination reactions (k_t) also occur in ATRP, mainly through radical coupling and disproportionation; however, in a well-controlled ATRP, no more than a few percent of the polymer chains undergo termination.

The rate of polymerization is first order with respect to monomer, alkyl halide (initiator), and transition metal complexed by ligand. The reaction is usually negative first order with respect to the deactivator ($X\text{-}M_t^{n+1}$/Ligand). The rate equation of copper-based ATRP is formulated in discussed conditions and given in (2.1). The apparent propagation rate constant, where k_p and K_{eq} refer to the absolute rate constant of propagation and the atom transfer equilibrium constant for the propagating species, respectively.

$$Rp = k_p^{app} (M) = k_p (R\bullet) (M) = k_p K_{eq} (I) ((CuX)/(CuX_2)) (M) \quad \textbf{(2.1)}$$

Figure 2.7 shows a typical linear variation of conversion with time in semi logarithmic coordinates (kinetic plot). Such a behavior indicates that there is a constant concentration of active species in the polymerization and first-order kinetics with respect to monomer.

However, since termination occurs continuously, the concentration of the Cu(II) species increases and deviation from linearity may be observed [33]. For the ideal case with chain length independent from termination, persistent radical effect [37] kinetics implies the semi logarithmic plot of monomer conversion vs. time to the 2/3 exponent should be linear. Nevertheless, a linear semi logarithmic plot is often observed.

This may be due to an excess of the Cu(II) species present initially, a chain length dependent termination rate coefficient, and heterogeneity of the reaction system due to limited solubility of the copper complexes. It is also possible that self-initiation may continuously produce radicals and compensate for termination. Similarly,

external orders with respect to initiator and the Cu(I) species may also be affected by he persistent radical effect [38].

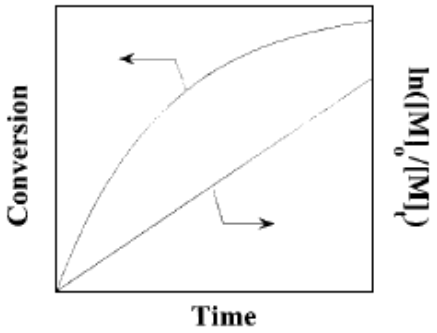

Figure 2.7 : Kinetic plot and conversion vs. time plot for ATRP.

Results from kinetic studies of ATRP for styrene (S) [39] methyl acrylate (MA) [40] and methyl methacrylate (MMA) [41, 42] under homogeneous conditions indicate that the rate of polymerization is first order with respect to monomer, initiator, and Cu(I) complex concentrations. These observations are all consistent with the derived rate law.

It should be noted that the optimum ratio can vary with regard to changes in the monomer, counter ion, ligand, temperature, and other factors [41, 43]. The precise kinetic law for the deactivator CuX_2 was more complex due to the spontaneous generation of Cu(II) via the persistent radical effect [38, 39].

In the atom transfer step, a reactive organic radical is generated along with a stable Cu(II) species that can be regarded as a persistent metallo-radical. If the initial concentration of deactivator Cu(II) in the polymerization is not sufficiently large to ensure a fast rate of deactivation (k_d(Cu(II)), then coupling of the organic radicals will occur, leading to an increase in the Cu(II) concentration.

Radical termination occurs rapidly until a sufficient amount of deactivator Cu(II) is formed and the radical concentration is low. Under such conditions, the rate at which radicals combine (k_t) will become much slower than the rate at which radicals react with the Cu(II) complex in a deactivation process and a controlled polymerization will proceed.Typically, a small fraction (~5 %) of the total growing polymer chains will be terminated during the early stage of the polymerization, but the majority of the chains (>95 %) will continue to grow successfully.

If the deactivation does not occur, or if it is too slow ($k_p >> k_d$), there will be no control and polymerization will become classical redox reaction therefore the termination and transfer reactions may be observed. To control the polymerization better, addition of one or a few monomers to the growing chain in each activation step is desirable. Molecular weight distribution for ATRP is given in (2.2).

$$M_w/M_n = 1 + ((k_d(RX)_0)/(k_p(X\text{-}M_t^{n+1}))) \times ((2/p)-1) \quad \textbf{(2.2)}$$

p = polymerization yield

$(RX)_o$ = concentration of the functional polymer chain

$(X\text{-}M_t^{n+1})$ = concentration of the deactivators

k_d = rate constant of deactivation

k_p = rate constant of activation

2.4.2 Components of ATRP

As a multicomponent system, ATRP includes the monomer, an initiator with a transferable (pseudo) halogen, and a catalyst (composed of a transition metal species with any suitable ligand). Both activating and deactivating components of the catalytic system must be simultaneously present. Sometimes an additive is used. For a successful ATRP, other factors, such as solvent and temperature, must also be taken into consideration.

2.4.2.1 Monomers

A variety of monomers have been successfully polymerized using ATRP: styrenes, (meth)acrylates, (meth)acrylamides, dienes, and acrylonitrile, which contain substituents that can stabilize the propagating radicals [36]. However, even under the same conditions using the same catalyst, each monomer has its own unique atom transfer equilibrium constant for its active and dormant species [44].

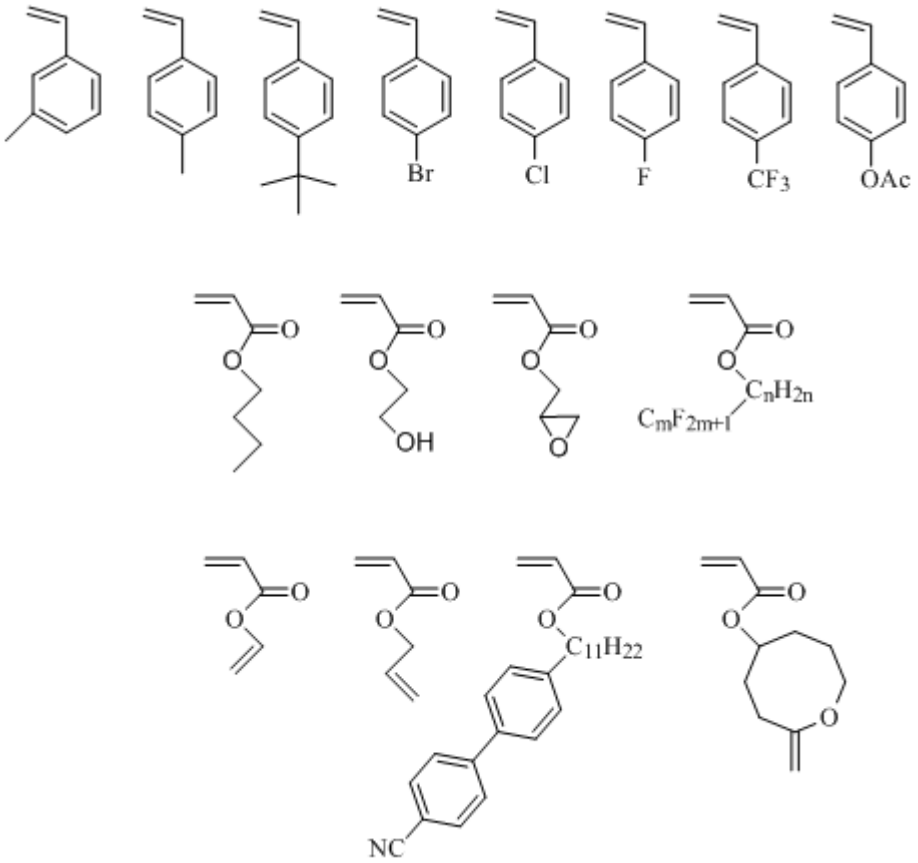

Figure 2.8 : Some of the monomers used in ATRP.

2.4.2.2 Initiators

Organic halides having a labile carbon-halogen bond are the most successfully employed initiators in ATRP. In general, these organic halides possess electron withdrawing groups and/or atoms such as carbonyl, aryl, cyano, or halogens at α-carbon to stabilize the generated free radicals. The common way to initiate is via the reaction of an activated (alkyl) halide with the transition-metal complex in its lower oxidation state. To obtain well-defined polymers with narrow molecular weight distributions, the halide atom, X, should rapidly and selectively migrate between the growing chain and the transition metal complex. Thus far, when X is either bromine or chlorine, the molecular weight control is best. Iodine works well for acrylate polymerizations in copper-mediated ATRP and has been found to lead to controlled polymerization of St in ruthenium and ruthenium-based ATRP [45-47].

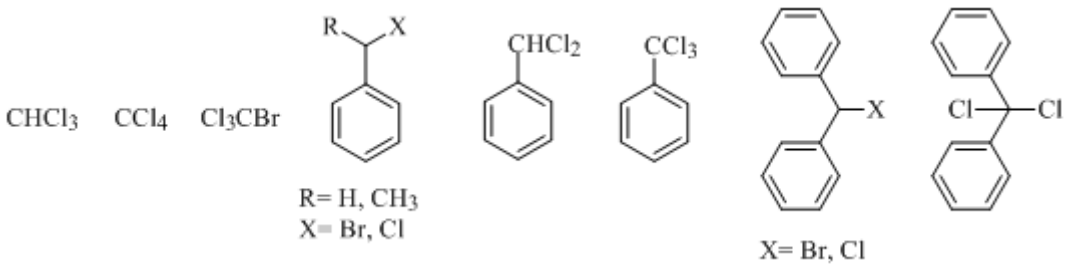

Figure 2.9 : ATRP initiators; halogenated alkanes and benzylic halides.

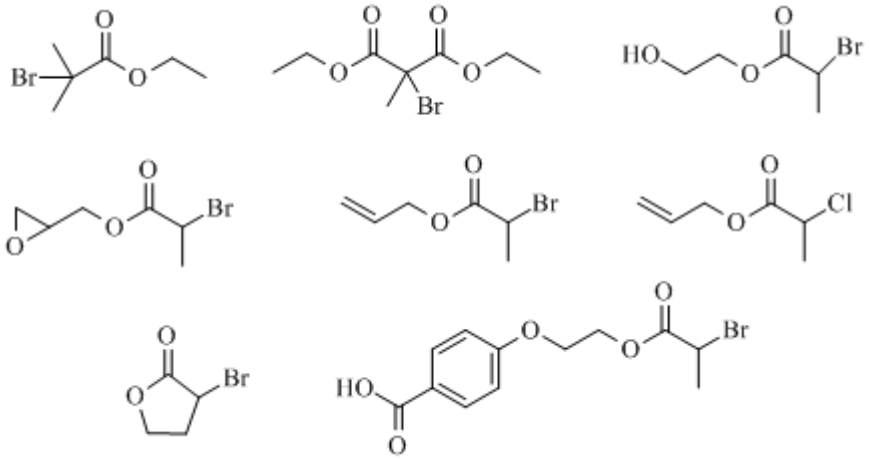

Figure 2.10 : ATRP initiators; α-bromoesters.

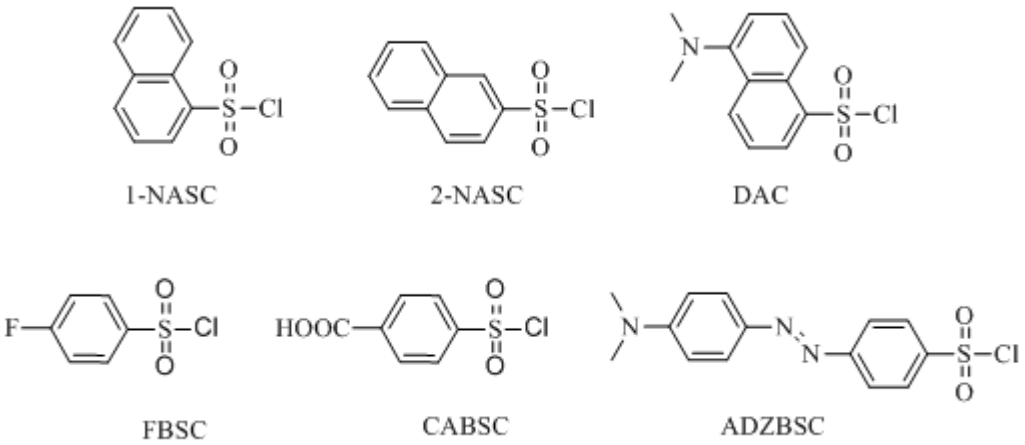

Figure 2.11 : ATRP initiators; sulfonyl chlorides.

2.4.2.3 Catalyst and transition metals

Perhaps the most important component of ATRP is the catalyst. It is the key to ATRP since it determines the position of the atom transfer equilibrium and the dynamics of exchange between the dormant and active species. There are several prerequisites for an efficient transition metal catalyst. The metal center must have at least two readily accessible oxidation states separated by one electron. The metal center should have reasonable affinity toward a halogen. The coordination sphere

around the metal should be expandable on oxidation to selectively accommodate a (pseudo) halogen. The ligand should complex the metal relatively strongly. Eventually, the position and dynamics of the ATRP equilibrium should be appropriate for the particular system. To differentiate ATRP from the conventional redox-initiated polymerization and induce a controlled process, the oxidized transition metal should rapidly deactivate the propagating polymer chains to form the dormant species. A variety of transition metal complexes with various ligands have been studied as ATRP catalysts. The majority of work on ATRP has been conducted using copper as the transition metal. Apart from copper-based complexes, Fe, Ni, Ru, etc. have been used to some extent [31, 33].

2.4.2.4 Ligands

The major roles of the ligand in ATRP is to solubilize the transition metal salt in the organic media and to adjust the redox potential and halogenophilicity of the metal center forming a complex with an appropriate reactivity and dynamics for the atom transfer. The ligand should complex strongly with the transition metal, should also allow expansion of the coordination sphere, and should allow selective atom transfer without promoting other reactions.

The most common ligands for ATRP systems are substituted bipyridines, alkyl pyridylmethanimines and multidentate aliphatic tertiary amines such as N,N,N′,N″,N″pentamethyldiethylenetriamine (PMDETA), and tris[2-(dimethylamino) ethyl]amine (Me_6-TREN) [48, 49]. In addition to those commercial products, it has been demonstrated that hexamethyltriethylene tetramine (HMTETA) provides better solubility of the copper complexes in organic media and entirely homogeneous reaction conditions [39]. Since copper complexes of this new ligand are almost insoluble in water, ATRP technique can be employed in preparing poly(acrylate esters) in aqueous suspensions.

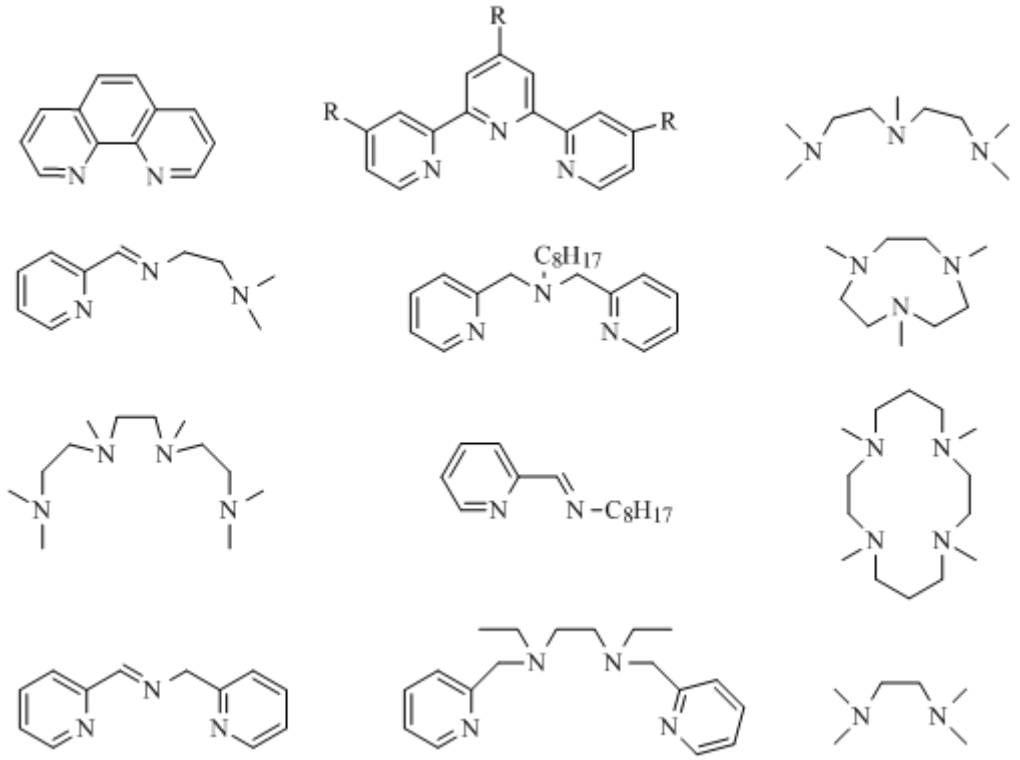

Figure 2.12 : Some of the ligands using ATRP.

2.4.2.5 Solvents

Solvents: ATRP can be carried out either in bulk, in solution, or in a heterogeneous system (e.g., emulsion, suspension). Various solvents, such as benzene, toluene, anisole, diphenyl ether, ethyl acetate, acetone, dimethyl formamide (DMF), ethylene carbonate, alcohol, water, carbon dioxide, and many others, have been used in the polymerization of different monomers.

2.4.2.6 Temperature and reaction time

The rate of polymerization in ATRP increases with increasing temperature due to the increase of both the radical propagation rate constant and the atom transfer equilibrium constant. As a result of the higher activation energy for the radical propagation than for the radical termination, higher k_p/k_t ratios and better control ("livingness") may be observed at higher temperatures. However, chain transfer and other side reactions become more pronounced at elevated temperatures. The optimal temperature depends mostly on the monomer, the catalyst, and the targeted molecular weight. Therefore, for successful ATRP, optimum temperature should be found depending on the monomer, catalyst and the other components of ATRP [33].

2.4.3 Reversible addition–fragmentation chain transfer process (RAFT)

Reversible addition-fragmentation chain transfer (RAFT) polymerization is one of the most efficient methods in C/LRP [50, 51]. The RAFT system consists of a small amount of RAFT agent and monomer and a free-radical initiator. Radicals stemming from the initiator are used at the very beginning of the polymerization to trigger the degenerative chain transfer reactions that dominate the polymerization. Free radicals affect both the molecular weight distribution of the polymer as the dead polymer chains of uncontrolled molecular weight are formed and the rate of polymerization. Therefore, the concentration of free radicals introduced in the system needs to be carefully balanced [52].

There are four classes of thiocarbonylthio RAFT agents, depending on the nature of the Z group: (1) dithioesters (Z = aryl or alkyl), (2) trithiocarbonates (Z = substituted sulfur), (3) dithiocarbonates (xanthates) (Z = substituted oxygen), and (4) dithiocarbamates (Z = substituted nitrogen). Representative examples of thiocarbonylthio RAFT agents are shown in Figure 2.1, where the Z group is the activating group, and R is the homolytically-leaving group. Largely, the Z group determines the rate of addition, and the R group determines the rate of fragmentation. The choice of Z and R groups is dependent on the nature of the monomer to be polymerized [53, 54].

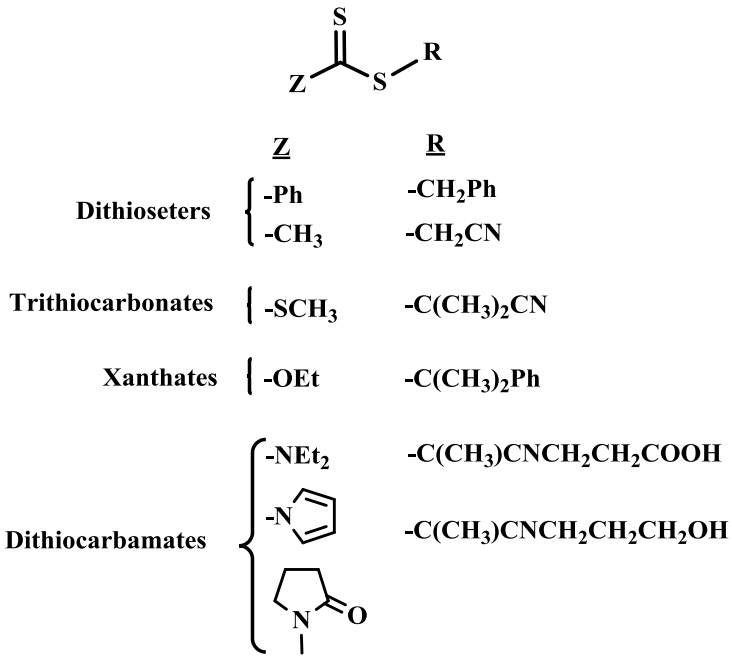

Figure 2.13 : Examples of the different classes of thiocarbonylthio RAFT agents.

The mechanism of RAFT polymerization with the thiocarbonylthio-based RAFT agents involves a series of addition–fragmentation steps as depicted in Figure 2.14. Initiation and radical–radical termination occur as in conventional radical polymerization. Initiation starts with decomposition of an initiator leads to formation of propagating chains. In the early stages of the polymerization, addition of a propagating radical (P_n•) to the to the thiocarbonylthio compound [S=C(Z)SR] followed by fragmentation of the intermediate radical gives rise to a polymeric RAFT agent and a new radical (R•). The radical R• reinitiates polymerization by reaction with monomer to form a new propagating radical (P_m•). In the presence of monomer, the equilibrium between the active propagating species (P_n• and P_m•) with the dormant polymeric RAFT compound provides an equal probability for all the chains to grow. This feature of the RAFT process offers the production of narrow polydispersity polymers. When the polymerization is complete, most of the chains retain the thiocarbonylthio end-group.

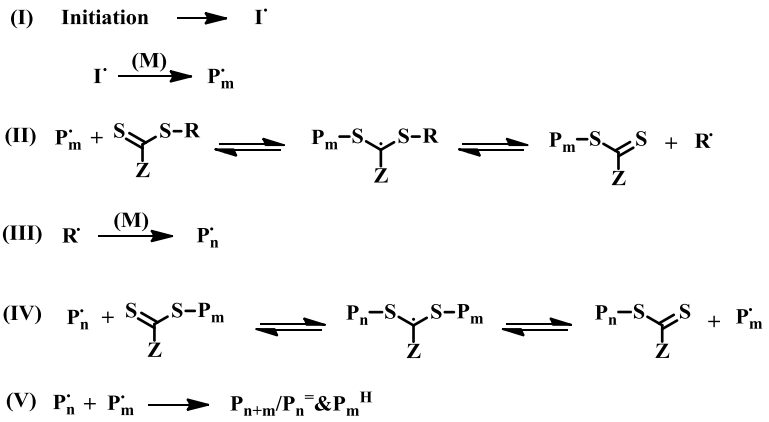

Figure 2.14 : Proposed general mechanism of RAFT polymerization.

In RAFT polymerization, radicals may be generated in three different ways: (1) by decomposition of organic initiators, (2) by the use of an external source (UV–vis or γ-ray), and (3) by thermal initiation. Polymerization temperature is usually in the range of 60–80 ^{o}C, which corresponds to the optimum decomposition temperature interval of the well-known initiator azobis(isobutyronitrile) (AIBN). However, even room temperature and high temperature conditions can also be applied [55, 56].

Photo- and γ-ray-induced reactions, which use light energy to generate radicals in RAFT polymerization, offer a number of advantages compared with thermally initiated ones. The major advantage is to allow the polymerization to be conducted at room temperature with relatively shorter reaction times. In photoinduced reactions,

however, the RAFT agent should carefully be selected, as in some cases control over the molecular weight cannot be attained, particularly at high conversions because it may also decompose under UV light [57]. RAFT polymerization induced by γ-Ray appeared to be more penetrating compared with the corresponding UV-induced processes.

2.4.4 Iniferter

Iniferters are initiators that induce radical polymerization that proceeds via initiation, propagation, primary radical termination, and transfer to initiator. These polymerizations are performed by the insertion of the monomer molecules into the iniferter bond, leading to polymers with two iniferter fragments at the chain ends, in addition, bimolecular termination and other transfer reactions are negligible. If the end groups of the polymers obtained by a suitable iniferter serve further as a polymeric iniferter, these polymerizations proceed by a living radical polymerization mechanism in a homogeneous system.

The iniferters are divided from the structure of their bonds into A-B type and C-C type iniferters as shown in Figure 2.15.

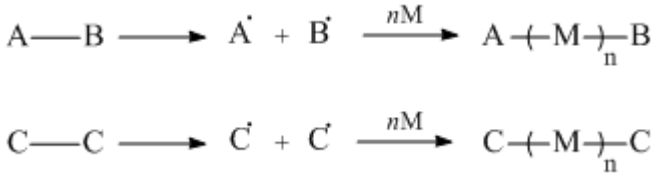

Figure 2.15 : Types of iniferters.

Where A^* is a reactive radicl that participates in initiation and then propagation, and B^* is a less reactive or nonreactive radical that principally enters into termination to give polymer. In the case of C-C type iniferters two C^* are less reactive radicals that participate in both initiation and termination, leading to polymer, in which *n* is the total number ofinserted monomer molecules.

2.5 Photopolymerization

Photopolymerization is one of the most rapidly expanding processes for materials production and is employed over a wide range of applications because of their advantages compare to traditional thermal polymerization. The use of light gives

solvent-free formulation, very high reaction rates at room temperature, low energy input to the polymerization system.

Photopolymerizations are initiated by light typically in the UV or visible region of the light spectrum by certain types of compounds which are capable of absorbing light of a particular wavelength. The range of wavelength is determined by the reactive system including the monomers, the initiators and any photosensitizers. An active center is produced when the initiator absorbs light and undergoes some type of decomposition, hydrogen abstraction or electron transfer reaction.

Photoiniferters such as N,N-diethyl dithiocarbamate (DDC) and its derivatives can be used in photopolymerization. Polymeric photoiniferters have low volatility and do not suffer from initiator migration effects. Polymeric photoiniferters can also be used as precursors for block and graft polymerization reactions. Several examples of the use of DDCs in this type of application have been recently reported.The use of a combination of living cationic polymerization and radical or controlled radical polymerization to prepare block copolymers has also been reported [58].

2.6 Polysulfone (PSf)

Polysulfones describe a family of thermoplastic polymers with their high glass transition temperature, thermal stability and chemical inertness. Polysulfone's chain rigidity, translated to its mechanical stability as a material, exists due to the relatively inflexible and immobile phenyl and SO_2 groups. The ether bonds allow PSf to be flexible and tough yet strong as shown in Figure 2.16. Due to these properties, PSf is widely used in the areas of material science, biology and polymer science. Commercial applications include carbon dioxide stripping from natural gas streams and the production of high purity nitrogen from air. In addition, polysulfones are used as ion exchange membranes in electromembrane processes, such as electrodialysis, and polymer electrolyte membrane electrolysis [59-61].

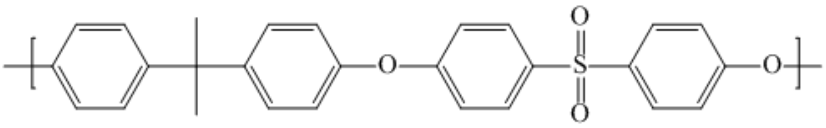

Figure 2.16 : Chemical structure of PSf

Despite PSf is a popular membrane because of good thermal and chemical stability, mechanical strenght and excellent oxidative resistance, the hydrophobic nature of PSf gives some limitation in membrane application. Thus, hydrophilic PSf membrane surfaces have created using a variety of methods including hydrophilic polymer coatings deposited [62-64]; hydrophilic layers graft polymerized onto polysulfone membranes using radical reactions generated with low-temperature plasma [65-67]; ultraviolet [68, 69] or gamma radiation [70]; chemical reaction of hydrophilic components onto the membrane surface or bulk PSf [6, 7].

For instance, sulfonyl and hudroxyl end-terminated groups are combined with PSf membrane surfaces by Higuchi and co-workers achieved reduced protein absorption compared to unmodified PSf [71]. Radiation technique is used to graft polymerize hydrophilic monomers such as acrylic acid, methacrylic acid and 2-hydroxy-ethyl methacrylate (HEMA) onto PSf membrane surface by Belfort and co-workers [72]. Another approach about modification of PSf is the chemical modification of bulk PSf using lithiation chemistry, incorporating hydrophilic components such as carboxylated and hydroxylated derivatives studied by Guiver et all [73].

3. EXPERIMENTAL PART

3.1 Chemicals

Polysulfone (PSf, M_n= 26000 g/mol) was donated by Solvay Advanced Polymers, 2-Acrylamido-2-methylpropan sulfonic acid (AMPS, Figure 3.1) was purchased from Lubrizol. Copper (I) bromide (CuBr, 98%), *tert*-butyl acrylate (*t*BA, 99%, Figure 3.2) and diethyldithiocarbomic acid sodium salt trihydrate (Figure 3.3) were purchased from Across Organics Co. *N*,*N*,*N*',*N*'',*N*''-Pentamethyldiethylenetriamine (PMDETA, 99%), paraformaldhyde (95%), chlorotrimethylsilane ($(CH_3)_3SiCl$), and hydrochloric asit (HCl, 37%) were purchased from Merck. 2-2'-bipyridine (bpy) was purchased from Fluka. Copper (I) chloride (CuCl, 99%), 3-sulfopropyl methacrylate potassium salt (SPMAK, 98%, Figure 3.3), trifluoroacetic acid (TFA, 99%) and tin (IV) chloride ($SnCl_4$) were purchased from Sigma-Aldrich. Methanol (MeOH ,technical purity) was purchased from Honeywell. 1-4-dioxanne, tetrahydrofuran (THF, 99.9%) and N,N-dimethylformamide (DMF, 99.8 %) were purchased from Labkim.

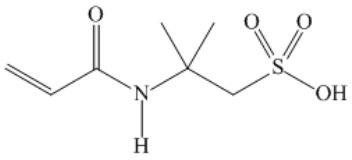

Figure 3.1 : 2-Acrylamido-2-methylpropan sulfonic acid (AMPS).

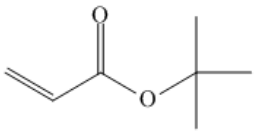

Figure 3.2 : *Tert*-butyl acrylate (*t*BA).

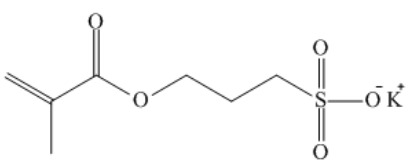

Figure 3.3 : 3-sulfopropyl methacrylate potassium salt (SPMAK).

3.2 Modification of PSf

3.2.1 Chloromethylation of PSf

PSf was chloromethylated by following procedures similar to those described by Avram and coworkers [74]. In a typical reaction, 33.6 mmol (14.88 g) of PSf was dissolved in 750 ml of chloroform in round bottom flask and mixture was stirred. Next, 336 mmol (10 g) of paraformaldehyde, 3.36 mmol (0.39 ml) of $SnCl_4$, and 336 mmol (42.5 ml) of $(CH_3)_3SiCl$ were added to PSf solution. A reflux condenser was then attached to the round bottom flask and placed in a heated bath. After three days at desired reaction temperature (30-60 ^oC), the reaction mixture was precipitated in methanol and polymers were isolated by filtration. The polymer was subsequently dissolved in chloroform and precipitated in methanol, then filtered and dried under vacuum overnight at 50 ^oC.

3.2.2 Synthesis of PSf-DDC (Polysulfone-diethyl dithiocarbomate)

PSf-DDC was synthesis from the reaction of PSf with sodium diethyl dithiocarbomate trihydrate. PSf (0.5 g), sodium diethyl dithiocarbomate (given amounth) and 50 mL DMF were placed to 100-mL flask in silicone oil bath. The reaction was continued under stirring for 6 hours at 60 ^oC. The solution was precipitated in methanol and polymer was isolated by filtration. For purification, polymer was dissolved in chloroform and reprecipitated in methanol then filtered and dried under vacuum at 50 ^oC.

3.2.3 AMPS functionalization of PSf by iniferter methods

Given amount of AMPS monomer and PSf-DDC were dissolved in 40 mL DMF and the solution was stirred though 20 minutes at room temperature. The solution was placed into the photoreactor tube and was nitrogen bubbled throughout 15 minutes before the tube was replaced in photoreactor at 25 ^oC. The reaction was maintained at 280 nm for different reaction times. Mixtures were precipitated in methanol and filtred. After filtration, polymers were dried for 24 hours in a vacuum at 50 ^oC.

3.2.4 SPMAK functionalization of PSf

CuBr as catalyst and PSf-CH_2Cl, were added into a 100 mL Schlenk flask and deoxygenated by three vacuum-nitrogen cycles, then mixture were dissolved with

addition of DMF followed by nitrogen bubbled 20 minutes. SPMAK solution in 5 mL of DMF and PMDETA were added to the flask, respectively. After 15 minutes nitrogen purging, the flask was replaced in thermostatically controlled oil bath at different temperatures. All liquids, i.e. monomer solution, ligand and solvent, were purged with nitrogen just before use. Different conditions of ATRP reactions at different ratios of the chemicals were carrried out. To control the reaction, alequot was taken via syringe from the reaction solution and were precipitated in methanol and filtered. After filtration, polymer samples were dried for 24 hours in a vacuum oven at 50 ^{o}C.

3.2.5 *t*BA functionalization of PSf

PSf-CH_2Cl and catalyst (CuBr or CuCl) were added into a 100 mL Schlenk flask and deoxygenated by three vacuum-nitrogen cycles, then mixture were dissolved with addition of DMF or Dioxan followed by nitrogen bubbled 20 minutes. *t*BA as monomer and PMDETA or bpy as ligand were added to the flask, respectively. After 15 minutes nitrogen purging, the flask was replaced in thermostatically controlled oil bath at different temperatures. All liquids, i.e. monomer, ligand and solvent, were purged with nitrogen just before use. Different conditions of ATRP reactions at different ratios of the chemicals were carrried out. To control the reaction, alequot was taken via syringe from the reaction solution and were precipitated in methanol and filtered. After filtration, polymer samples were dried for 24 hours in a vacuum oven at 50 ^{o}C.

3.2.6 Hydrolysis of PSf-*t*BA

Obtained PSf-*t*BA was hydrolized by trifluoroacetic acid in chloroform for 18 hours. Then mixture was precipitated in metanol, filtered and dried in vacuum oven at 50 ^{o}C for 1 day.

3.3 Characterization Methods

3.3.1 Infrared spectrometer (FT-IR)

FT-IR spectra were recorded on a Thermo Nicolet 6700 FT-IR spectrometer.

3.3.2 Differential scanning calorimetry (DSC)

Differential scanning calorimetry (DSC, Figure 3.4) measurements were done to find out glass transition temperature (T_g) values using TA instruments Q1000 series. All tests were carried out under 50 ml.min^{-1} rate of nitrogen purge. All T_g measurement were investigated on TA Universal Analysis software by the inflection of change in the endothermic direction of the heating ramp.

Figure 3.4 : Differential scanning calorimetry (DSC, TA Q1000).

3.3.3 Nuclear magnetic resonance spectroscopy (NMR)

^{1}H NMR measurements (Figure 3.5) were recorded in $CDCl_3$ and DMSO-d6, using an Agilent VNMRS500 (500 MHz) instrument.

Figure 3.5 : Agilent VNMRS500 NMR insturment.

3.3.4 Electrochemical impedance spectroscopy (EIS)

Electrochemical impedance spectroscopic (Figure 3.6) measurements were conducted at room temperature (25 ^{o}C) using the conventional three electrode cell configuration. The electrochemical cell was connected to a potentiostat (Parstat

2263-1), which interfaced to a computer. An electrochemical impedance software (Powersine) was used to carry out impedance measurements by scanning in the 10 - 100 kHz frequency range with applied AC signal amplitude of 10 mV. The impedance spectra were analyzed using AC impedance data analysis software (ZSimpWin V3.10).

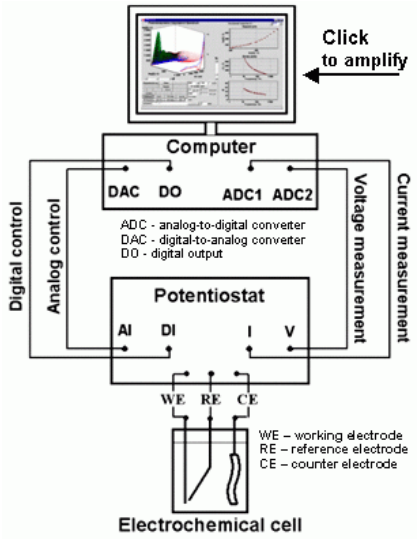

Figure 3.6 : General diagram of electrochemical impedance spectroscopy.

4. RESULTS AND DISCUSSION

4.1 Modification of PSf

4.1.1 Chlorometylation of PSf

To obtain PSf based graft copolymer by ATRP, macroinitiator PSf-CH_2Cl was synthesized by chlorometylation of PSf according to Figure 4.1.

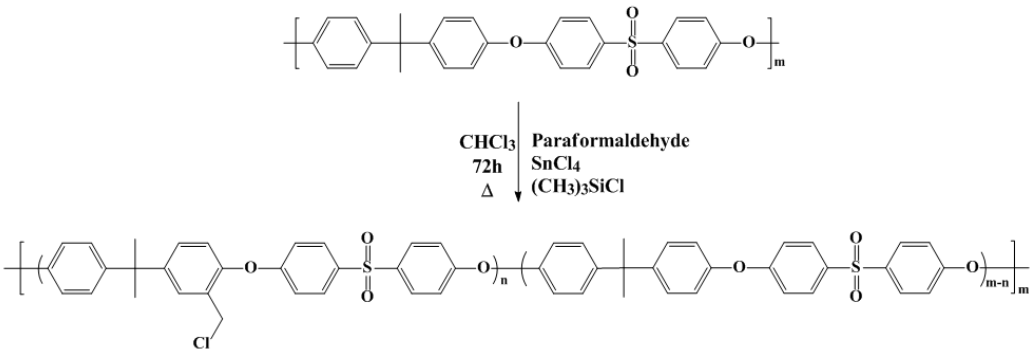

Figure 4.1 : Synthesis of chloromethylated PSf.

After purifying PSf-CH_2Cl, ^{1}H-NMR measurement was applied in order to determine degree of substitution of chloromethyl group in PSf. A representative NMR spectrum of 60% chloromethylated PSf was shown in Figure 4.2.

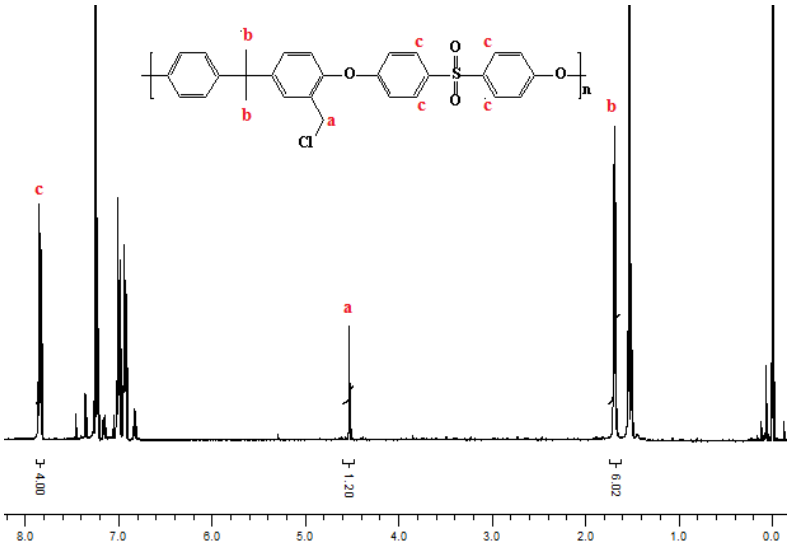

Figure 4.2 : ^{1}H-NMR spectrum of PSf-CH_2Cl-60 in $CDCl_3$.

As can be seen from Figure 4.2, six hydrogens of -CH_3 group (b) of PSf-CH_2Cl are appeared at 1.7 ppm, two hydrogens of -CH_2Cl group (a) of PSf-CH_2Cl are appeared at 4.53 ppm and four hydrogens of acidic hydrogen of benzene (c) are appeared at 7.8 ppm. Degree of substitution of chloromethyl group into PSf backbone was calculated relative integral ratio for corresponding groups as mentioned above.

Table 4.1 shows content % of chloromethylated groups in PSf backbones and reaction conditions.

Table 4.1 : Chloromethylation of PSf[a].

Run	Temperature (^oC)	Degree of substition
PSf-CH_2Cl-60	50	0.60
PSf-CH_2Cl-33	50	0.33
PSf-CH_2Cl-37[b]	30	0.37

[a] [PSf]:[Paraformaldehyde]:[$(CH_3)_3SiCl$]:[$SnCl_4$]= 1:10:10:0.1. PSf=$2.2x10^{-2}$ mol, paraformaldehyde=$2.2x10^{-1}$ mol, $SnCl_4$=$2.2x10^{-3}$ mol $(CH_3)_3SiCl$=$2.2x10^{-1}$ mol, at 50 ^oC in 250 mL of chloroform.

[b] [PSf]:[Paraformaldehyde]:[$(CH_3)_3SiCl$]:[$SnCl_4$]= 1:10:10:0.5. PSf=$2.2x10^{-2}$ mol, paraformaldehyde=$2.2x10^{-1}$ mol, $SnCl_4$=$1.1x10^{-2}$ mol $(CH_3)_3SiCl$=$2.2x10^{-1}$ mol, at 30 ^oC in 250 ml of chloroform.

4.1.2 Synthesis of PSf-DDC

To ionic group incorporation into PSf, iniferter method was used. Therefore, PSf containing iniferter agent DDC (PSf-DDC), which is the precursor for AMPS grafted PSf, was synthesized by the reaction of PSf-CH_2Cl and sodium diethyl dithiocarbamate according to the Figure 4.3.

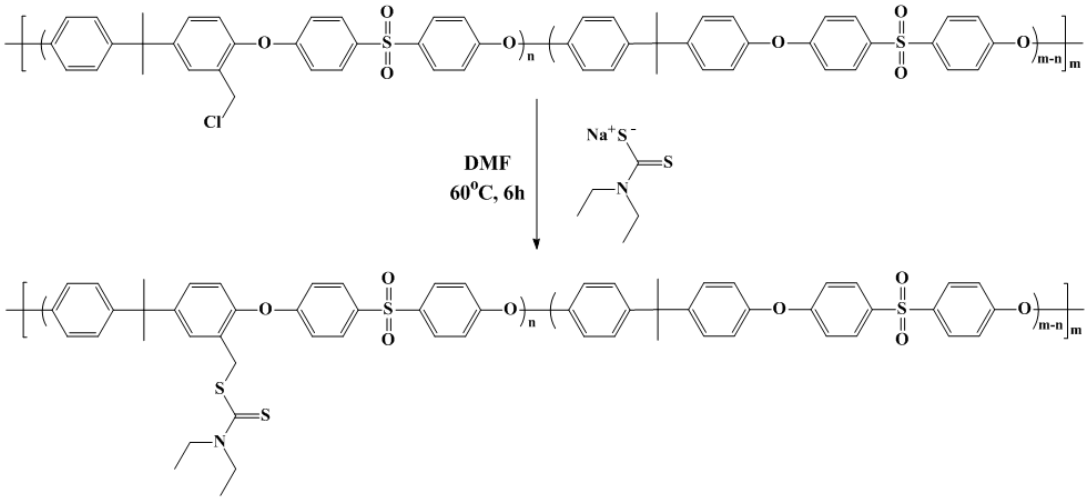

Figure 4.3 : The synthesis of PSf-DDC.

The successful synthesis of PSf-DDC was confirmed by ^{1}H-NMR. As can be seen in Figure 4.4 for PSf-DDC-60, six hydrogens of -CH_3 group (b) of DDC are appeared at 1.2 ppm and four hydrogens of -N(CH_2) groups (a) of DDC are appeared between 3.5-3.9 ppm.

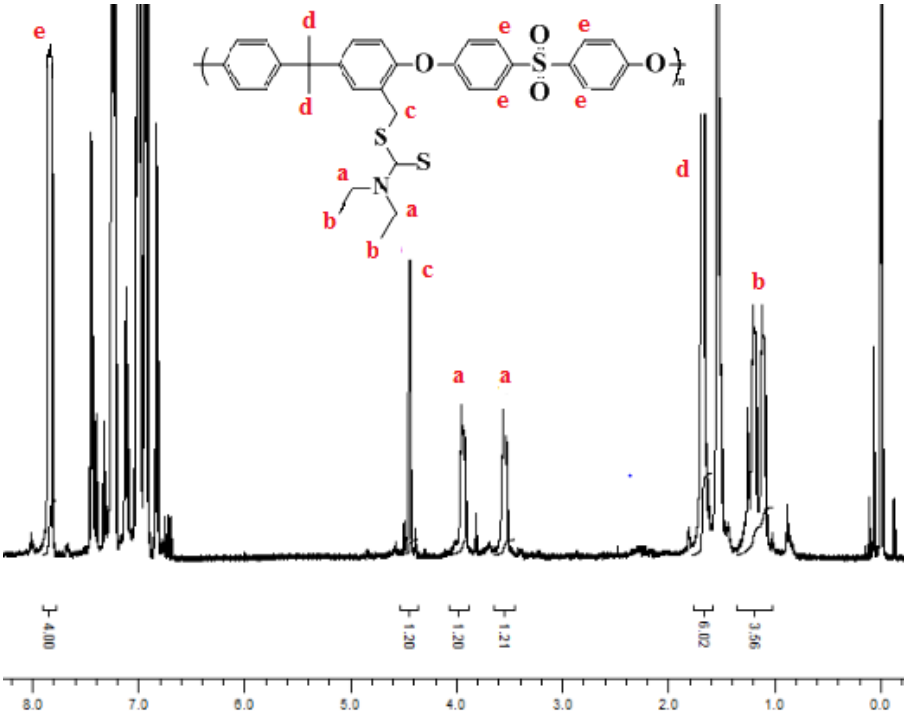

Figure 4.4 : ^{1}H-NMR spectrum of PSf-DDC-60 in DMSO-d6.

The reaction conditions of PSf-DDC and results were shown in Table 4.2. When amount of DDC was used in reaction lower than amount of chloride content, the conversion occured lower than expected. However, complete conversion was obtained thereby using equal amount DDC with chloride content.

Table 4.2 : The synthesis of PSf-DDC[a].

Run	**PSf-CH_2Cl**		**[DDC]/[PSf-CH_2Cl]**	
	Type	Eq. mole	Feed	Found
PSf-DDC-60	PSf-CH_2Cl-60	$6.3x10^{-4}$	1	1
PSf-DDC-27	PSf-CH_2Cl-60	$6.3x10^{-4}$	0.40	0.31
PSf-DDC-20	PSf-CH_2Cl-60	$6.3x10^{-4}$	0.55	0.41
PSf-DDC-33	PSf-CH_2Cl-33	$0.7x10^{-4}$	1	1

[a] 60 ^{o}C, 6 hours in 50 mL DMF.

4.1.3 AMPS functionalization of PSf by iniferter method

To obtain PSf-based amphiphilic copolymer, PSf-*g*-AMPS, iniferter polymerization of AMPS was carried out using PSf-DDC by 280 nm light (Figure 4.5).

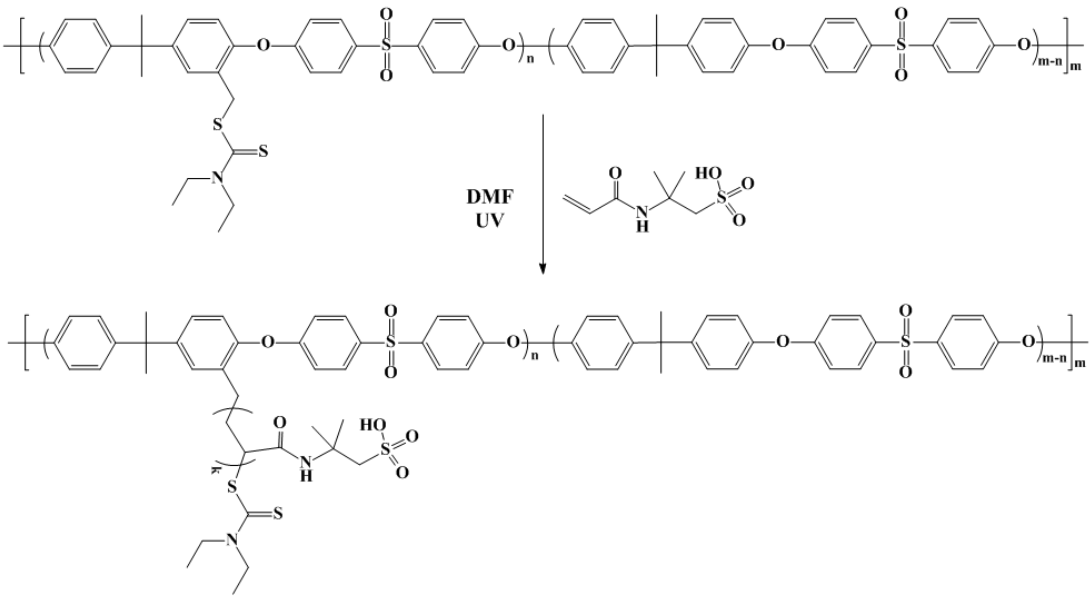

Figure 4.5 : Synthesis of AMPS grafted PSf (PSf-*g*-AMPS) by iniferter method.

Reaction conditions and results for the reaction of different types of PSf-DDC and AMPS were tabulated in Table 4.3.

Table 4.3 : The synthesis of PSf-*g*-AMPS[a].

PSf-DDC		**AMPS**	Time (h)	AMPS graft[b]
Type	Eq. mole	mole		
PSf-DDC-60	$1.8x10^{-4}$	$1.1x10^{-4}$	6	x-link
PSf-DDC-60	$3.7x10^{-4}$	$2.2x10^{-4}$	5	x-link
PSf-DDC-60	$3.7x10^{-4}$	$2.2x10^{-4}$	4	x-link
PSf-DDC-60	$3.7x10^{-4}$	$2.2x10^{-4}$	3	x-link
PSf-DDC-60	$3.7x10^{-4}$	$2.2x10^{-4}$	2	0 %
PSf-DDC-60	$3.7x10^{-4}$	$2.2x10^{-4}$	1.5	0 %
PSf-DDC-33	$9.2x10^{-4}$	$6.6x10^{-5}$	2	0 %
PSf-DDC-33	$8.5x10^{-4}$	$6.6x10^{-5}$	2	0 %
PSf-DDC-33	$2.1x10^{-4}$	$6.6x10^{-5}$	2	0 %
PSf-DDC-27	$2.0x10^{-3}$	$5.3x10^{-5}$	3	0 %
PSf-DDC-27	$2.0x10^{-3}$	$5.3x10^{-5}$	2	0 %
PSf-DDC-27	$8.0x10^{-4}$	$5.3x10^{-5}$	1.5	0 %
PSf-DDC-20	$2.0x10^{-3}$	$4.0x10^{-5}$	2	0 %
PSf-DDC-20	$8.0x10^{-4}$	$4.0x10^{-5}$	2	0 %

[a] λ_{max}= 280 nm at 25 ^{o}C in 40 mL DMF.
[b] Measured by ^{1}H-NMR.

Iniferter polymerization of AMPS were accomplished for long reaction time i.e. 6 h, 5 h, 4 h or 3 h, x-link was monitored. Besides, AMPS grafted PSf backbone was not observed even for short reaction time of iniferter polymerization according to NMR measurement.

4.1.4 SPMAK functionalization of PSf

PSf-CH_2Cl as macroinitiator and SPMAK as monomer was used in ATRP method to obtain SPMAK grafted PSf (PSf-*g*-SPMAK). Synthesis reaction of PSf-*g*-SPMAK via ATRP method is shown in Figure 4.6.

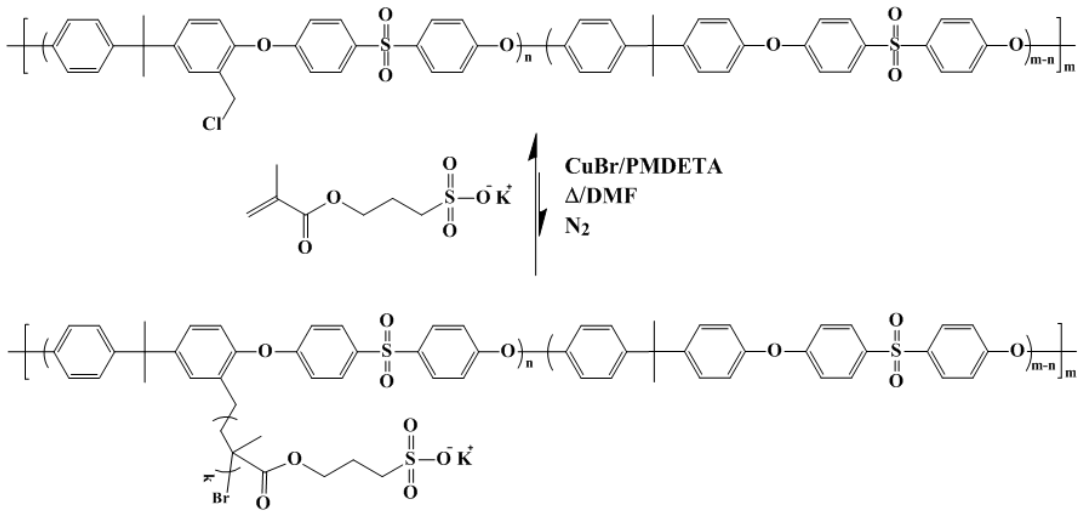

Figure 4.6 : Synthesis of PSf-*g*-SPMAK.

ATRP of SPMAK was carried out with different reaction conditions (Table 4.4) and effects of these conditions were monitored by FT-IR and ^{1}H-NMR.

The monomer addition to PSf backbone was not observed according to FT-IR and NMR mesurement for 30 ^oC for 15 min. Then x-link polymers were obtained for different ATRP ratios and different initiator types for 1.5 h at 30 ^oC (Run 2 and 3) and at 50 ^oC (Run 4 and 5). On the other hand, monomer addition was monitored beside the residual monomer by FT-IR measurement and NMR for Run 6 (Figure 4.7 and Figure 4.8), Run 7. Therefore, the polymers were dissolved in chloroform and reprecipitation in MeOH, filtred and dried. Due to the fact that polymer was not dissolved any solvent after re-purification, x-link polymers were observed. Although monomer addition was also detected by FT-IR, composition was not defined by ^{1}H-NMR due to obtained polymer was x-linked for Run 8.

Table 4.4 : Reaction conditions of PSf-*g*-SPMAK by ATRP.

Run	Initiator (I)		[SPMAK]/[I]/[PMDETA]/[CuBr]	T (^{o}C)	Time (h)
	Type	Eq. mole			
1	PSf-CH_2Cl-60	$1.2x10^{-3}$	0.8/1/0.4/0.4	30	0.25
2	PSf-CH_2Cl-60	$1.2x10^{-3}$	0.8/1/0.4/0.4	30	1.5
3	PSf-CH_2Cl-33	$3.6x10^{-4}$	1/1/0.5/0.5	30	1.5
4	PSf-CH_2Cl-37	$4.0x10^{-4}$	20/1/0.3/0.3	50	1.5
5	PSf-CH_2Cl-33	$3.6x10^{-4}$	4/1/1/1	50	1.5
6	PSf-CH_2Cl-60	$6.3x10^{-4}$	0.9/1/0.5/0.4	50	1.5
7	PSf-CH_2Cl-60	$6.3x10^{-4}$	0.9/1/0.5/0.4	70	1.5
8	PSf-CH_2Cl-60	$1.2x10^{-3}$	0.8/1/0.4/0.4	90	0.08

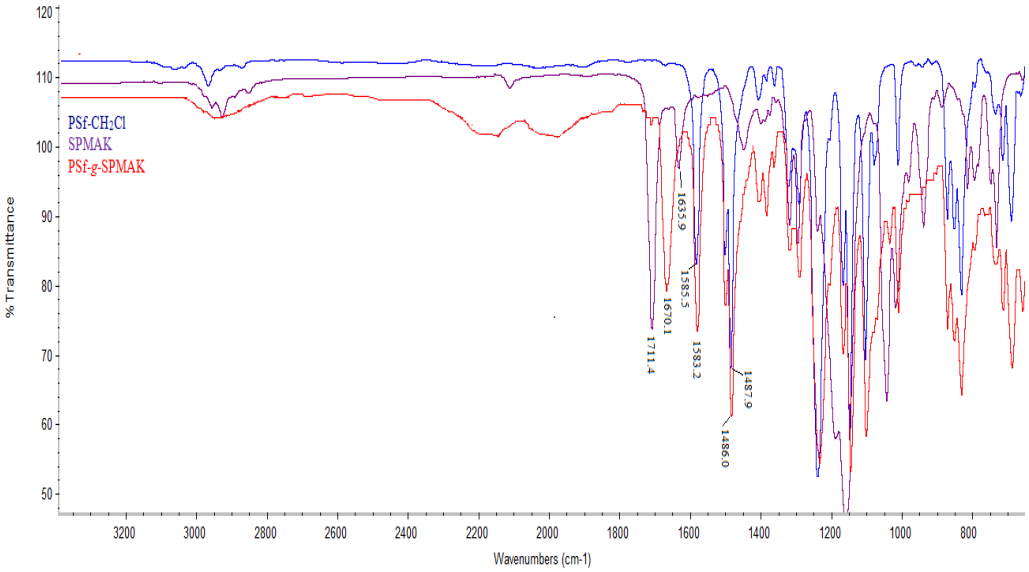

Figure 4.7 : IR spectrum of PSf-CH_2Cl-60, SPMAK and PSf-*g*-SPMAK.

It can be seen that in Figure 4.7, C=C double bond conjugated with C=O at 1635 cm^{-1} and C=O conjugated with C=C double bond at 1711 cm^{-1} for SPMAK. Whereas, a new peak at 1670 cm^{-1} in PSf-*g*-SPMAK, belonging to only the carbonyl group C=O, is clearly shows that the SPMAK was grafted to PSf backbone, i.e. conjugation was disappeared.

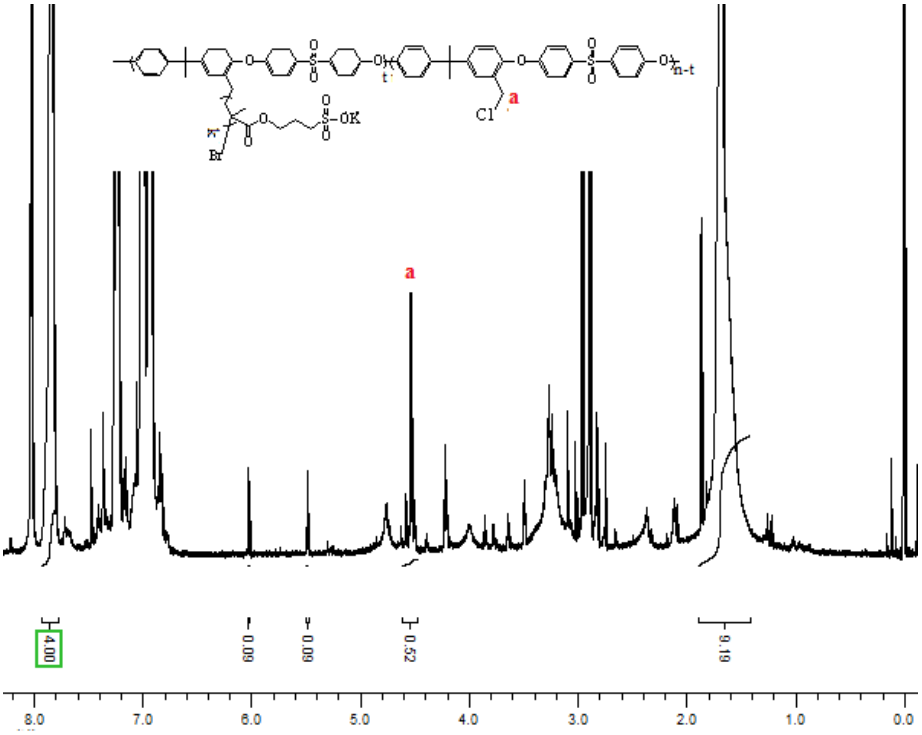

Figure 4.8 : ^{1}H-NMR spectrum of PSf-*g*-SPMAK in $CDCl_3$.

PSf-CH_2Cl-60 which contains 60 % of chlorometyhlated group in PSf backbone was used as macroinitiator, with integration area of two hydrogens of -CH_2Cl group was 1.20. As can be seen from Figure 4.8, the integration area of two hydrogens decreased from 1.20 to 0.52, means content % of chloromethylated group was diminished by monomer addition in PSf backbone. However, correct calculation of content % of SPMAK in PSf backbone was restrained because of monomer residual. After purification, x-link polymers were also designated.

4.1.5 *t*BA functionalization of PSf

PSf-CH_2Cl as macroinitiator and *t*BA as monomer was used in ATRP method to obtain *t*BA grafted PSf (PSf-*g*-*t*BA). The PSf-*g*-*t*BA was modified to include hydrophilic ionic moieties obtained by hydrolysis with TFA at 50 ^{o}C. The hydrolysis of PSf-*g*-*t*BA resulted in hydrophilic acrylic acid grafted PSf (PSf-*g*-AA). The steps of PSf-*g*-AA synthesis are shown in Figure 4.9.

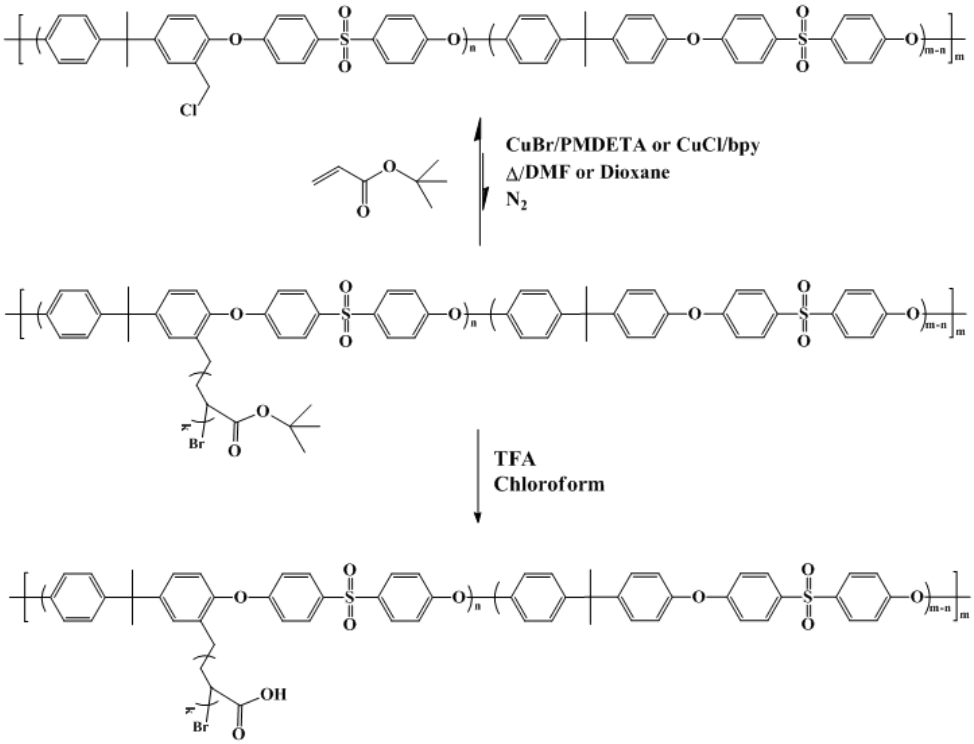

Figure 4.9 : Synthesis of PSf-*g*-AA.

ATRP of *t*BA was carried out with different reaction conditions (Table 4.5) and effects of these conditions were monitored by FT-IR and ^{1}H-NMR.

Table 4.5 : Reaction conditions of PSf-*g*-*t*BA by ATRP[a].

Run	Initiator		Ligand/Metal	[M]/[I]/[L]/[Me]	Time (h)	*t*BA/PSf[d]
	Type	Eq. mole				
1[b]	PSf-CH_2Cl-33	$3.2x10^{-4}$	PMDETA/CuBr	3/1/0.5/0.25	48	x-link
2[b]	PSf-CH_2Cl-33	$3.2x10^{-4}$	PMDETA/CuBr	3/1/0.5/0.25	24	x-link
3[c]	PSf-CH_2Cl-33	$3.2x10^{-4}$	Bpy/CuCl	20/1/1/1	18	0.16
4[c]	PSf-CH_2Cl-33	$3.2x10^{-4}$	Bpy/CuCl	20/1/1/1	48	0.34
5[c]	PSf-CH_2Cl-60	$6.2x10^{-4}$	Bpy/CuCl	20/1/1/1	96	1.16
6[c]	PSf-CH_2Cl-60	$6.2x10^{-4}$	Bpy/CuCl	20/1/1/1	144	1.38

[a] In 20 mL DMF
[b] At 80 ^{o}C
[c] At 90 ^{o}C
[d] Measured by ^{1}H-NMR

Bpy/CuCl was used in ATRP due to the fact that polymerization reaction was fast with PMDETA/CuBr. FT-IR spectras of PSf-CH_2Cl, PSf-*g*-*t*BA and PSf-*g*-AA were represented in Figure 4.10. A strong absorption at 1729 cm^{-1} belongs to C=O stretching of carboxylic acid group of PSf-*g*-*t*BA shifted to 1710 cm^{-1}.

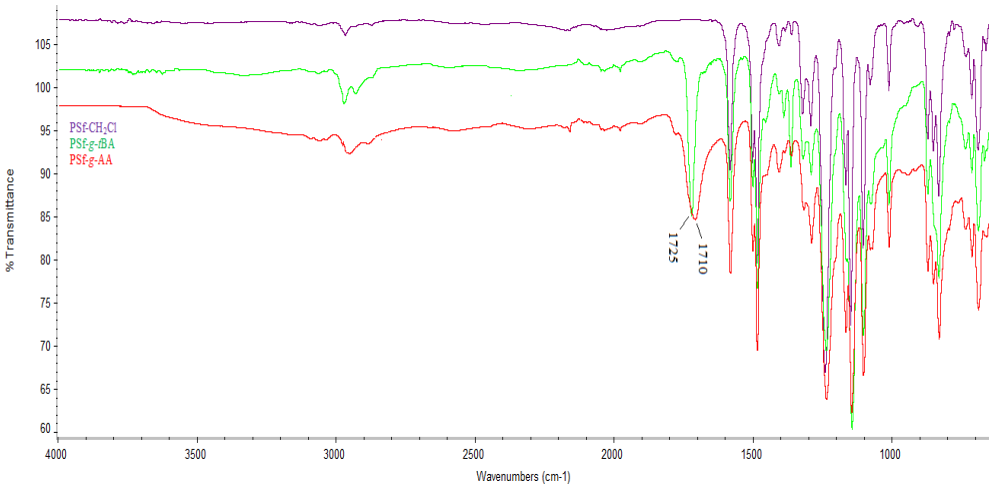

Figure 4.10 : FT-IR spectrum of PSf-*g*-AA.

A representetive NMR spectrum of PSf-*g*-*t*BA using Bpy/CuCl complex was shown in Figure 4.11 (Run 6). The pure PSf-CH_2Cl spectrum exhibits a well-known peaks in the regions 7.8 ppm for four hydrogens of benzene, 4.54 ppm for two hydrogens of -CH_2Cl group and 1.7 ppm for six hydrogens of -CH_3 group (as can be seen in Figure 4.2). Grafting of *t*BA to PSf resulted in the appearance of peaks in the region 1.3-1.5 ppm due to protons of tert butyl group bonding, also dissappearance of peaks in the region 4.54 ppm.

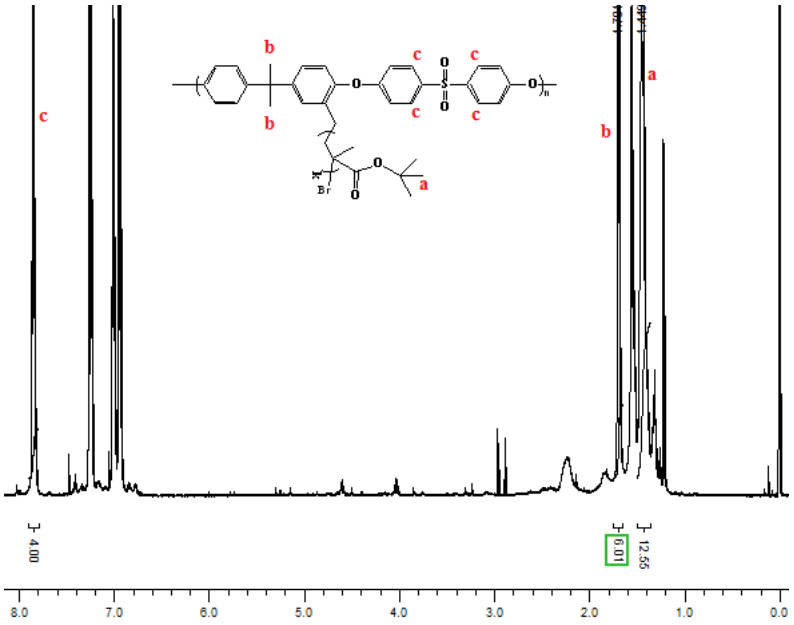

Figure 4.11 : ^{1}H-NMR spectrum of PSf-*g*-*t*BA in $CDCl_3$.

The NMR spectrum from the hydrolyzed product shows the disappearance of the *t*-butyl group in 1.4 ppm (Figure 4.12).

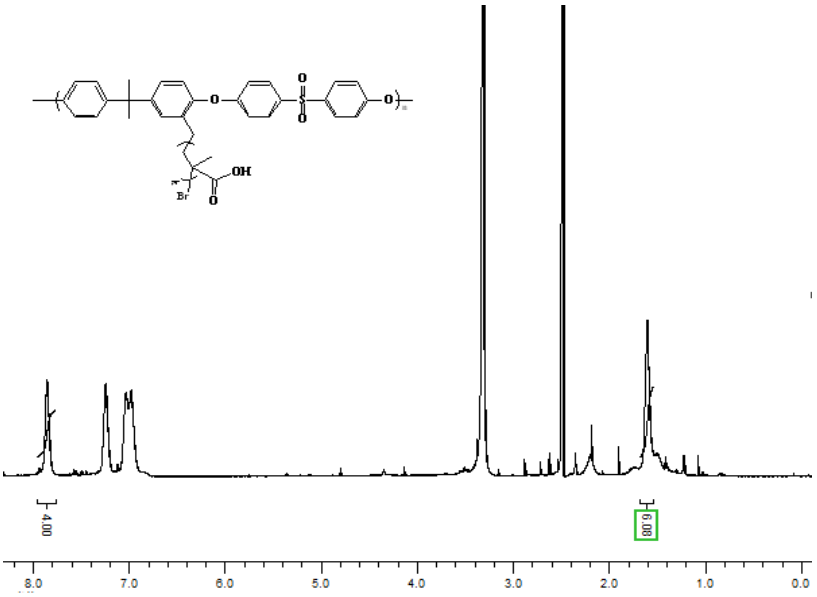

Figure 4.12 : ^{1}H-NMR spectrum of PSf-*g*-AA in DMSO-d6.

After NMR and FT-IR, thermal behavior of PSf-*g*-AA was investigated by using differantial scanning calorimetry in order to see T_g values of the pure PSf and also the obtained materials (Figure 4.13). For PSf and PSf-CH_2Cl-60, samples were heated from 0 to 250 ^{o}C. After first heating cycle, materials were cooled to 0 ^{o} C. For second heating cycle, samples were also heated again from 0 to 250 ^{o}C.

First cycle heating (from 0 to 200 ^{o}C) was chosen for PSf-*g*-*t*BA and PSf-*g*-AA due to the fact that both of which decomposed at second cycle heating.

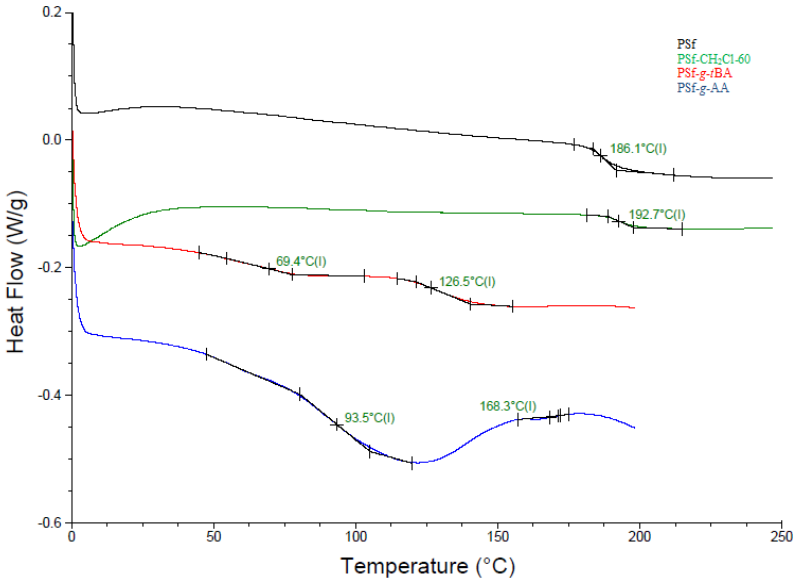

Figure 4.13 : DSC curves of PSf and PSf-CH_2Cl-60 (second heating cycle); PSf-*g*-*t*BA and PSf-*g*-AA (first heating cycle).

As can be seen from DSC curve of PSf, its T_g value is 186.1 ^oC, increasing for chloromethyl functionalized PSf backbone. As for PSf-*g*-*t*BA, an additional glass transition temperature (T_g), which should be attributed to *t*BA graft groups, can be found at 69.4 ^oC due to the inserted pattern and also decreased in T_g value of PSf-CH_2Cl were monitored. After hydrolysis, T_g values changed into 93.5 ^oC, corresponding to AA and 168.3 ^oC as to PSf-C_2Cl.

Table 4.6 : T_g values of pure PSf and obtained polymers.

Sample	T_g (^oC)
PSf	186.1
PSf-CH_2Cl-60	192.7
PSf-*g*-*t*BA	69.4 ; 126.5
PSf-*g*-AA	93.5 ; 168.3

Ion conductivity of pure PSf and its derivatives were determined by using Electrochemical Impedance Spectroscopy (EIS). Samples were prepared as 10^{-2} M solution in DMF. After the EIS measurements, obtained nyquist graph and magnetude graph were presented in Figure 4.14 and Figure 4.15, respectively .

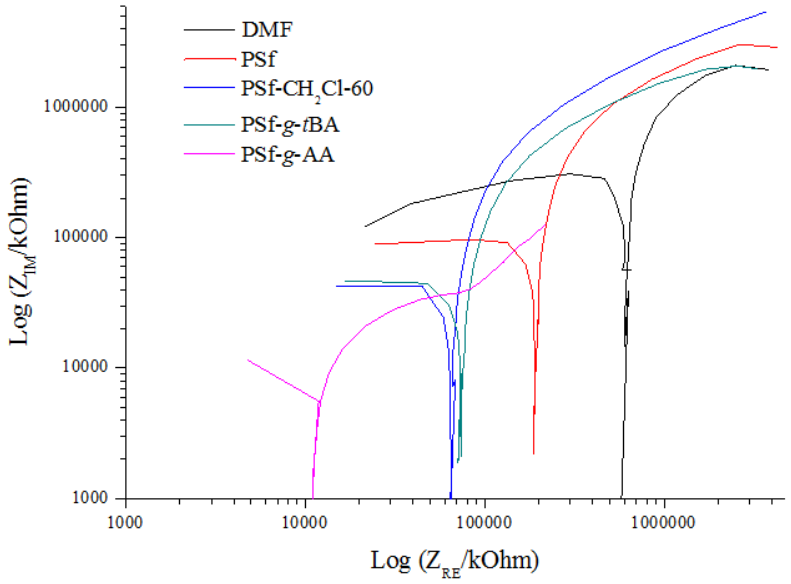

Figure 4.14 : Nyquist graph of EIS measurements.

X scale of the nyquist graph shows the resistance of the solution. Where, it can be clearly seen that DMF has higher resistance unlike PSf-*g*-AA have lower resistance. These results are shown PSf-*g*-AA solution have ion conductivity.

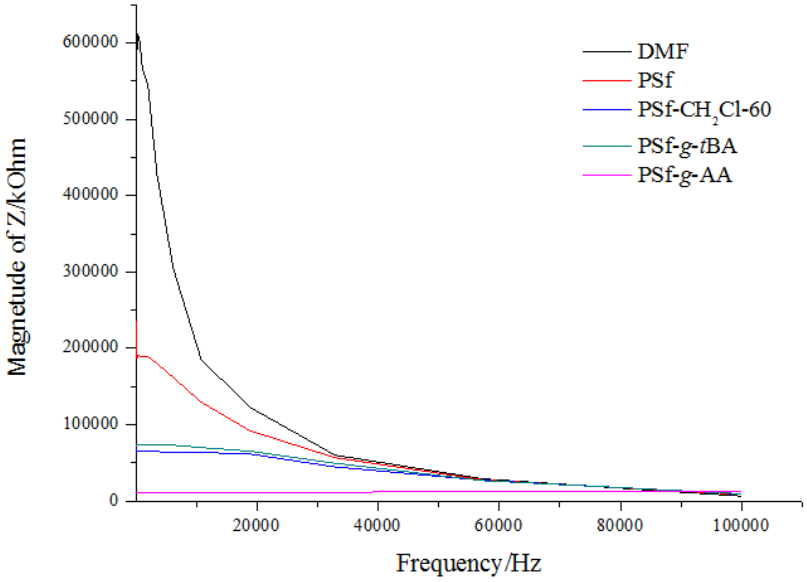

Figure 4.15 : Magnetude graph of EIS measurements.

In contrast to the nyquist graph, y scale of the magnitude graph shows the resistance and according to Figure 4.15, it can be seen that PSf-*g*-AA have again lower resistance than other solutions. Just as nyquist graph, these results is also shown that PSf-*g*-AA solution have ion conductivity.

5. CONCLUSION

In the development of new proton exchange membranes (PEM) for fuel cells, functionalization of a polymer offers many advantages, in particular with respect to the mechanical properties and the price of the material. Functionalization is possible with graft or block copolymerization.

The first aim of this study was to develop alternative membranes that have suitable thermal and chemical stability, comparable proton conductivity and relatively low cost compare the Nafion® products. In this respect, PSf was choosen as backbone alternative because of good thermal and chemical stability, mechanical strenght and excellent oxidative resistance. On the other hand, the hydrophobic nature of PSf gives some limitation in membrane application. Thus, hydrophobic PSf membrane surfaces have functionalized by iniferter method and ATRP. For this purpose, chloromethylated PSf (PSf-CH_2Cl) was synthesized firstly. Therefore, PSf containing iniferter agent DDC (PSf-DDC), which is the precursor for AMPS grafted PSf, was synthesized by the reaction of PSf-CH_2Cl and sodium diethyl dithiocarbamate. Then, PSf-DDCs containing different content % of DDC were used as macrophotoinitiator in order to synthesized PSf-*g*-AMPS via iniferter polymerization at 280 nm. After characterized by FT-IR and NMR measurements, addition of AMPS to PSf backbone was not observed.

Secondly, PSf-*g*-SPMAK was synthesized via ATRP by using different type of PSf-CH_2Cl as macroinitiator and at different temperatures, but solubility problems were occured.

Lastly, PSf-CH_2Cl as macroinitiator and *t*BA as monomer was used in ATRP method to obtain *t*BA grafted PSf (PSf-*g*-*t*BA). PSf-*g*-*t*BA was hydrolized to include hydrophilic moiety obtained with TFA at 50 ^oC. The hydrolysis of PSf-*g*-*t*BA resulted in hydrophilic acrylic acid grafted PSf (PSf-*g*-AA) which was characterized by NMR and FT-IR. Thermal properties of PSf-*g*-AA was investigated by using DSC measurements. The main aim of this study was to synthesize proton conductive polymer. For this purpose, ion conductivity of the material was investigated by using

electrochemical impedance spectroscopy (EIS). Increase in ion conductivity of PSf-*g*-AA solution compare to PSf-CH_2Cl and PSf-*g*-*t*BA was demostrated by nyquist and magnetude graph obtained by EIS.

Next step of this study can be to prepare of PSf-*g*-AA films and to compare with conventional fuel cell membranes in terms of advantages and disadvantages.

REFERENCES

[1] Pimentel, D. And Pimentel, M. H. (2008). *Food, Energy, and Society*, Taylor & Francis Group, Boca Raton.

[2] Vasquez, L. O. (2007). *Fuel Cell Research Trends*, Nova Science Publishers, Inc., New York.

[3] John Twidell, T. W. (2006). *Renewable Energy Resources*, Taylor & Francis, New York.

[4] Schuster, M. F. H. and Meyer, W. H. (2003). Anhydrous Proton-Conducting Polymers, *Annual Review of Materials Research*, *33*, 233-261.

[5] Richard, P., Zhigang, Q., Qunhui, G., Leng, M., John, F. E. and Bin, D. (2007). *Materials for Proton Exchange Membrane Fuel Cells*, CRC Press, pp. 251-309.

[6] Higuchi, A. and Nakagawa, T. (1990). Surface modified polysulfone hollow fibers. III. Fibers having a hydroxide group, *Journal of Applied Polymer Science*, *41*, 1973-1979.

[7] Higuchi, A., Ishida, Y. and Nakagawa, T. (1993). Surface modified polysulfone membranes: Separation of mixed proteins and optical resolution of tryptophan, *Desalination*, *90*, 127-136.

[8] Al-Kaabi, K. and van Reenen, A. J. (2008). Controlled radical polymerization of poly(methyl methacrylate-g-epichlorohydrin) using N,N-dithiocarbamate-mediated iniferters, *Journal of Applied Polymer Science*, *108*, 2528-2534.

[9] Sauguet, L., Boyer, C., Ameduri, B. and Boutevin, B. (2006). Synthesis and Characterization of Poly(vinylidene fluoride)-g-poly(styrene) Graft Polymers Obtained by Atom Transfer Radical Polymerization of Styrene, *Macromolecules*, *39*, 9087-9101.

[10] Beuscher, U., Cleghorn, S. J. C. and Johnson, W. B. (2005). Challenges for PEM fuel cell membranes, *International Journal of Energy Research*, *29*, 1103-1112.

[11] James Larminie, A. D. (2003). *Fuel Cell Systems Explained*, John Wiley&Sons Ltd., Chichester.

[12] Wu, J., Yuan, X. Z., Martin, J. J., Wang, H., Zhang, J., Shen, J., Wu, S. and Merida, W. (2008). A review of PEM fuel cell durability: Degradation mechanisms and mitigation strategies, *Journal of Power Sources*, *184*, 104-119.

[13] Rama, P., Chen, R. and Andrews, J. (2008). A review of performance degradation and failure modes for hydrogen-fuelled polymer

electrolyte fuel cells, *Proceedings of the Institution of Mechanical Engineers Part a-Journal of Power and Energy, 222*, 421-441.

[14] Cleghorn, S. J. C., Mayfield, D. K., Moore, D. A., Moore, J. C., Rusch, G., Sherman, T. W., Sisofo, N. T. and Beuscher, U. (2006). A polymer electrolyte fuel cell life test: 3 years of continuous operation, *Journal of Power Sources, 158*, 446-454.

[15] Drew Dunwoody, J. L. (2005). Proton Exchange Membranes: The View Forward and Back, *The Electrochemical Society Interface*.

[16] Thomas, G. J. and Jones, R. H. (2008). Materials for the Hydrogen Economy, *Materials for Proton Exchange Membrane Fuel Cells*.

[17] Manahan, S. E. (2001). *Fundamentals of Environmental Chemistry*, CRC Press LLc, Boca Raton.

[18] Adachi, M. (2004). in *Proton Exchange Membrane Fuel Cells: Water Permeation Through Nafion® Membranes*, Simon Fraser University.

[19] Achara, N. (2011). Fuel Cell Types and Characterization, *Nature and Science, 9*.

[20] D. Wheeler, G. S. (2008). in *2007 Status of Manufacturing: Polymer Electrolyte Membrane (PEM) Fuel Cell*, National Renewable Energy Laboratory.

[21] Url-1<http://www.h- tec.com>, retrieved date 25.01.2014

[22] Sorrell, C. C., Sugihara, S. and Nowotny, J. (2005). *Materials for energy conversion devices*, Woodhead, Cambridge.

[23] Harrison, W. L. (2002). in *Synthesis and Characterization of Sulfonated Poly(arylene ether sulfone) Copolymers via Direct Copolymerization: Candidates for proton Exchange Membrane Fuel Cell*, Virginia Polytechnic Institute, Virginia.

[24] Jianfu Ding, C. C., Steven Holdcroft. (2002). Enhanced Conductivity in Morphologically Controlled Proton Exchange Membranes: Synthesis of Macromonomers by SFRP and Their Incorporation into Graft Polymers, *Macromolecules, 35*.

[25] J. M. Serpico, S. G. E., J. J. Fontanella, X. Jiao, D. Perahia, and K. A. McGrady, E. H. S., G. E. Kellogg, G. E. Wnek. (2002). Transport and Structural Studies of Sulfonated Styrene-Ethylene Copolymer Membranes, *Macromolecules, 35*.

[26] Kreuer, K. D. (1997). Fast proton conductivity: A phenomenon between the solid and the liquid state?, *Solid State Ionics, 94*, 55-62.

[27] Szwarc, M. (1956). Living Polymers, *Nature, 178*, 1168, 1169.

[28] Michael Szwarc, M. B. (1993). *Ionic Polymerization and Living Polymers*, Chapman & HalI.

[29] Litvinenko, G. and Muller, A. H. E. (1997). General kinetic analysis and comparison of molecular weight distributions for various mechanisms of activity exchange in living polymerizations, *Macromolecules, 30*, 1253-1266.

[30] Masaaki Miyamoto, M. S., Toshinobu Higashimura. (1984). Living Polymerization of Isobutyl Vinyl Ether with the Hydrogen Iodide/Iodine Initiating System, *Macromolecules, 17*, 265-268.

[31] Masami Kamigaito, T. A., Mitsuo Sawamoto. (2001). Metal-Catalyzed Living Radical Polymerization, *Chemical Reviews, 101*, 3689−3745.

[32] Url-2<http://www.cmu.edu/maty/about-atrp.html>, retrieved date 12.12.2013.

[33] Matyjaszewski, K. and Xia, J. (2001). Atom Transfer Radical Polymerization, *Chemical Reviews, 101*, 2921-2990.

[34] Patten, T. E. (1998). Atom transfer radical polymerization and the synthesis of polymeric materials, *Advanced materials (Weinheim), 10*, 901.

[35] Patten, T. E., Xia, J., Abernathy, T. and Matyjaszewski, K. (1996). Polymers with Very Low Polydispersities from Atom Transfer Radical Polymerization, *Science, 272*, 866-868.

[36] Patten, T. E. (1999). Copper (I)-catalyzed atom transfer radical polymerization, *Accounts of chemical research, 32*, 895.

[37] Fischer, H. (1997). The Persistent Radical Effect In "Living" Radical Polymerization, *Macromolecules, 30*, 5666-5672.

[38] Shipp, D. A. and Matyjaszewski, K. (2000). Kinetic Analysis of Controlled/"Living" Radical Polymerizations by Simulations. 2. Apparent External Orders of Reactants in Atom Transfer Radical Polymerization, *Macromolecules, 33*, 1553-1559.

[39] Matyjaszewski, K., Patten, T. E. and Xia, J. (1997). Controlled/"Living" Radical Polymerization. Kinetics of the Homogeneous Atom Transfer Radical Polymerization of Styrene, *Journal of the American Chemical Society, 119*, 674-680.

[40] Davis, K. A., Paik, H.-j. and Matyjaszewski, K. (1999). Kinetic Investigation of the Atom Transfer Radical Polymerization of Methyl Acrylate, *Macromolecules, 32*, 1767-1776.

[41] Wang, J.-L., Grimaud, T. and Matyjaszewski, K. (1997). Kinetic Study of the Homogeneous Atom Transfer Radical Polymerization of Methyl Methacrylate, *Macromolecules, 30*, 6507-6512.

[42] Percec, V., Barboiu, B. and Kim, H. J. (1998). Arenesulfonyl Halides: A Universal Class of Functional Initiators for Metal-Catalyzed "Living" Radical Polymerization of Styrene(s), Methacrylates, and Acrylates†, *Journal of the American Chemical Society, 120*, 305-316.

[43] Percec, V., Barboiu, B., Neumann, A., Ronda, J. C. and Zhao, M. (1996). Metal-Catalyzed "Living" Radical Polymerization of Styrene Initiated with Arenesulfonyl Chlorides. From Heterogeneous to Homogeneous Catalysis, *Macromolecules, 29*, 3665-3668.

[44] Queffelec, J., Gaynor, S. G. and Matyjaszewski, K. (2000). Optimization of Atom Transfer Radical Polymerization Using Cu(I)/Tris(2-(dimethylamino)ethyl)amine as a Catalyst, *Macromolecules, 33*, 8629-8639.

[45] Wang, Y. and Huang, J. (1998). Controlled Radical Copolymerization of Styrene and the Macromonomer of PEO with a Methacryloyl End Group, *Macromolecules*, *31*, 4057-4060.

[46] Kotani, Y., Kamigaito, M. and Sawamoto, M. (2000). Living Radical Polymerization of Para-Substituted Styrenes and Synthesis of Styrene-Based Copolymers with Rhenium and Iron Complex Catalysts1, *Macromolecules*, *33*, 6746-6751.

[47] Kotani, Y., Kamigaito, M. and Sawamoto, M. (1999). Re(V)-Mediated Living Radical Polymerization of Styrene:1 ReO2I(PPh3)2/R−I Initiating Systems, *Macromolecules*, *32*, 2420-2424.

[48] Wang, J.-S. and Matyjaszewski, K. (1995). Controlled/"living" radical polymerization. atom transfer radical polymerization in the presence of transition-metal complexes, *Journal of the American Chemical Society*, *117*, 5614-5615.

[49] Haddleton, D. M., Jasieczek, C. B., Hannon, M. J. and Shooter, A. J. (1997). Atom Transfer Radical Polymerization of Methyl Methacrylate Initiated by Alkyl Bromide and 2-Pyridinecarbaldehyde Imine Copper(I) Complexes, *Macromolecules*, *30*, 2190-2193.

[50] Barner-Kowollik, C. (2008). *Handbook of RAFT Polymerization*, Wiley-VCH Verlag GmbH & Co. KGaA.

[51] Chiefari, J., Chong, Y. K., Ercole, F., Krstina, J., Jeffery, J., Le, T. P. T., Mayadunne, R. T. A., Meijs, G. F., Moad, C. L., Moad, G., Rizzardo, E. and Thang, S. H. (1998). Living Free-Radical Polymerization by Reversible Addition−Fragmentation Chain Transfer: The RAFT Process, *Macromolecules*, *31*, 5559-5562.

[52] Moad, G., Rizzardo, E. and Thang, S. H. (2008). Toward Living Radical Polymerization, *Accounts of Chemical Research*, *41*, 1133-1142.

[53] Moad, G., Rizzardo, E. and Thang, S. H. (2006). Living Radical Polymerization by the RAFT Process—A First Update, *Australian Journal of Chemistry*, *59*, 669-692.

[54] Moad, G., Rizzardo, E. and Thang, S. H. (2009). Living Radical Polymerization by the RAFT Process – A Second Update, *Australian Journal of Chemistry*, *62*, 1402-1472.

[55] Convertine, A. J., Ayres, N., Scales, C. W., Lowe, A. B. and McCormick, C. L. (2004). Facile, Controlled, Room-Temperature RAFT Polymerization of N-Isopropylacrylamide†, *Biomacromolecules*, *5*, 1177-1180.

[56] Quinn, J. F., Rizzardo, E. and Davis, T. P. (2001). Ambient temperature reversible addition-fragmentation chain transfer polymerisation, *Chemical Communications*, 1044-1045.

[57] Quinn, J. F., Barner, L., Barner-Kowollik, C., Rizzardo, E. and Davis, T. P. (2002). Reversible Addition−Fragmentation Chain Transfer Polymerization Initiated with Ultraviolet Radiation, *Macromolecules*, *35*, 7620-7627.

[58] Guan, J. and Yang, W. (2000). Photografting of PVC containing N,N-diethyldithiocarbamate groups with vinyl monomers, *Journal of Applied Polymer Science*, *77*, 2569-2574.

[59] Guiver, M. D., Robertson, G. P. and Foley, S. (1995). Chemical Modification of Polysulfones II: An Efficient Method for Introducing Primary Amine Groups onto the Aromatic Chain, *Macromolecules*, *28*, 7612-7621.

[60] Lau, W. W. Y. and Jiang, Y. (1994). Performance of polysulfone/carboxylated polysulfone membranes, *Polymer International*, *33*, 413-417.

[61] Kerres, J., Cui, W. and Reichle, S. (1996). New sulfonated engineering polymers via the metalation route. I. Sulfonated poly(ethersulfone) PSU Udel® via metalation-sulfination-oxidation, *Journal of Polymer Science Part A: Polymer Chemistry*, *34*, 2421-2438.

[62] Brink, L. E. S., Elbers, S. J. G., Robbertsen, T. and Both, P. (1993). The anti-fouling action of polymers preadsorbed on ultrafiltration and microfiltration membranes, *Journal of Membrane Science*, *76*, 281-291.

[63] Kim, K. J., Fane, A. G. and Fell, C. J. D. (1988). The performance of ultrafiltration membranes pretreated by polymers, *Desalination*, 70, 229-249.

[64] Higuchi, A., Sugiyama, K., Yoon, B. O., Sakurai, M., Hara, M., Sumita, M., Sugawara, S.-i. and Shirai, T. (2003). Serum protein adsorption and platelet adhesion on pluronic™-adsorbed polysulfone membranes, *Biomaterials*, *24*, 3235-3245.

[65] Wavhal, D. S. and Fisher, E. R. (2002). Hydrophilic modification of polyethersulfone membranes by low temperature plasma-induced graft polymerization, *Journal of Membrane Science*, *209*, 255-269.

[66] Song, Y.-Q., Sheng, J., Wei, M. and Yuan, X.-B. (2000). Surface modification of polysulfone membranes by low-temperature plasma–graft poly(ethylene glycol) onto polysulfone membranes, *Journal of Applied Polymer Science*, *78*, 979-985.

[67] Iwata, H., Ivanchenko, M. I. and Miyaki, Y. (1994). Preparation of anti-oil stained membrane by grafting polyethylene glycol macromer onto polysulfone membrane, *Journal of Applied Polymer Science*, 54, 125-128.

[68] Kilduff, J. E., Mattaraj, S., Pieracci, J. P. and Belfort, G. (2000). Photochemical modification of poly(ether sulfone) and sulfonated poly(sulfone) nanofiltration membranes for control of fouling by natural organic matter, *Desalination*, *132*, 133-142.

[69] Pieracci, J., Crivello, J. V. and Belfort, G. (2002). Increasing membrane permeability of UV-modified poly(ether sulfone) ultrafiltration membranes, *Journal of Membrane Science*, *202*, 1-16.

[70] Mok, S., Worsfold, D. J., Fouda, A. and Matsuura, T. (1994). Surface modification of polyethersulfone hollow-fiber membranes by γ-ray irradiation, *Journal of Applied Polymer Science*, *51*, 193-199.

[71] Higuchi, A., Mishima, S. and Nakagawa, T. (1991). Separation of proteins by surface modified polysulfone membranes, *Journal of Membrane Science*, *57*, 175-185.

[72] Ulbricht, M. and Belfort, G. (1996). Surface modification of ultrafiltration membranes by low temperature plasma II. Graft polymerization onto polyacrylonitrile and polysulfone, *Journal of Membrane Science*, *111*, 193-215.

[73] Guiver, M. D., Black, P., Tam, C. M. and Deslandes, Y. (1993). Functionalized polysulfone membranes by heterogeneous lithiation, *Journal of Applied Polymer Science*, *48*, 1597-1606.

[74] Avram, E., Butuc, E., Luca, C. and Druta, I. (1997). Polymers with Pendant Functional Group. III. Polysulfones Containing Viologen Group, *Journal of Macromolecular Science, Part A*, *34*, 1701-1714.

CURRICULUM VITAE

Name Surname: Buket ALKAN

Place and Date of Birth: Zonguldak/15.02.1987

Address: Emniyetevler Mah. Yeşilkıbrıs Sok. Dursun Bey Apt. No:3 D:8 4 Levent/İstanbul

E-Mail: bkt_alkan@hotmail.com

B.Sc.: Chemist/Istanbul Technical University

Professional Experience and Rewards:

Professional Experience,

- Organizing committee member; International Controlled/Living Polymerization Symposium, 2014, Antalya, Turkey (Co-charmens: Prof. Metin H. ACAR and Krzystof Matyjaszewski)
- Internship; Tisan Engineering Plastics Co. Ltd., Production Department (11/07/2011-05/08/2011)
- Internship; ITU Chemistry Department, MERG Group, Prof. Dr. Metin H. Acar Laboratory Experience (02/08/2010-27/08/2010)
- Internship; Eczacıbaşı-Baxter Hospital Supply Inc., Quality Control Department Laboratory Experience (05/07/2010-30/07/2010)

Rewads,

- Istanbul Technical University, Chemistry Department, 3rd Prize in Bachelor Thesis Poster Contest (2011).

PUBLICATIONS/PRESENTATIONS ON THE THESIS

- **Acar, M. H.,** Alkan, B., Basdal, M., Tas, C.E., Designing of Fuel Cell Membranes, *2013 Collaborative Conference on 3D&Materials Research (CC3DMR),* June 24-28, Jeju, Korea.

- Acar, M. H., **Alkan, B.**, The Effect of Stirring Rate on ATRP of Styrene, *44th World Chemistry Congress (IUPAC 2013),* August 11-16, Istanbul, Turkey.

- Acar, M. H., **Alkan, B.**, Polysulfone-Based Amphiphilic Polymers, *3rd International Symposiums on Controlled/ Living Polymerization (CLP'14)*, May 1-4, 2014, Antalya, Turkey.